Numerical Modelling of transcritical fluid behaviour using Lattice Boltzmann method

S. Gunasekaran

TUDelft
Delft
University of
Technology

Challenge the future
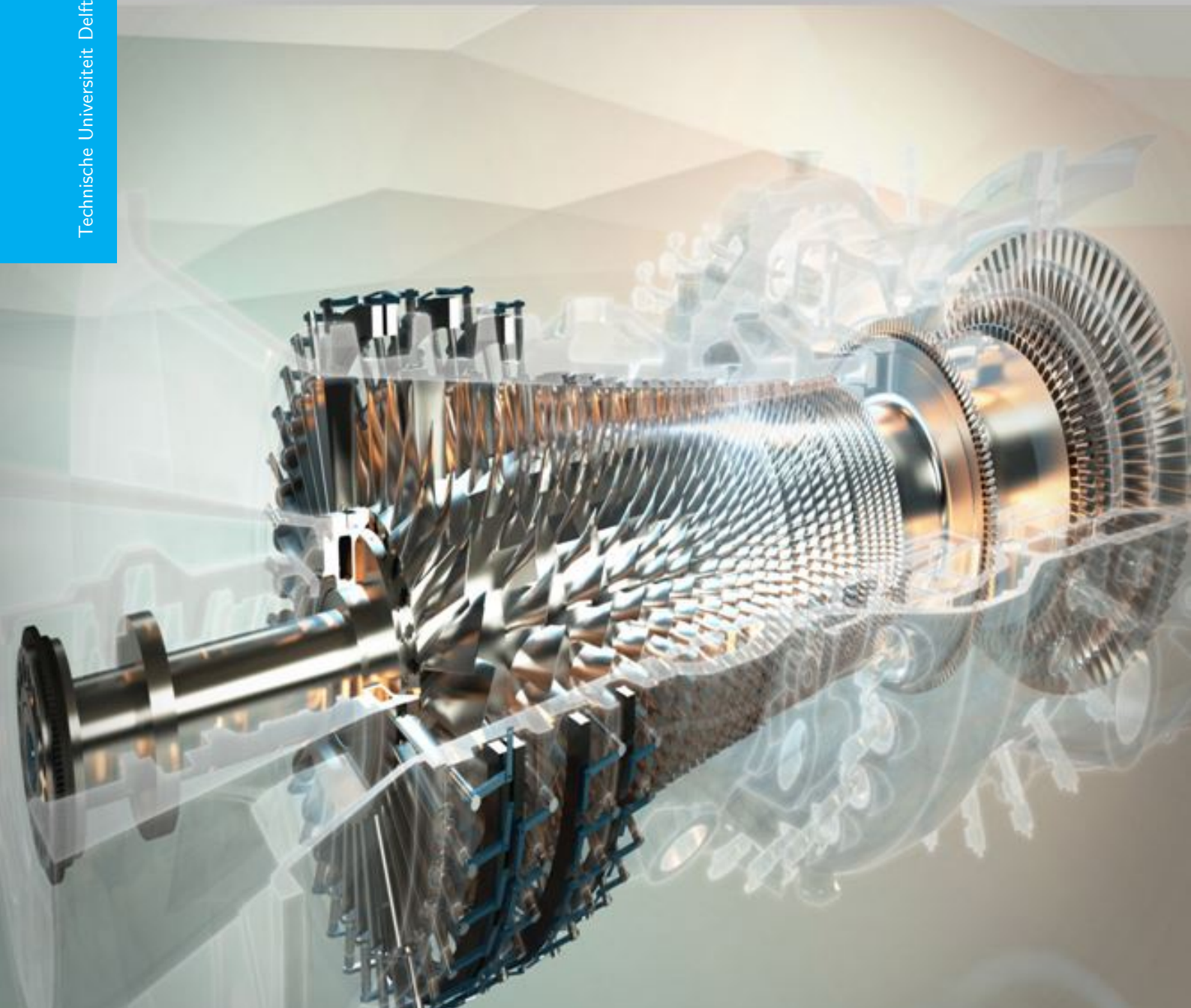
Numerical Modelling of transcritical fluid behaviour using Lattice Boltzmann method

by

S. Gunasekaran

in partial fulfillment of the requirements for the degree of

Master of Science
in Aerospace Engineering

at the Delft University of Technology,
to be defended publicly on Friday November 29, 2017 at 10:00 AM.

Supervisor:	Assistant Prof. Dr. ir. C. Lettieri	
Thesis committee:	Prof. Dr. ir. P. Colonna,	Power and Propulsion Group TU Delft
	Assistant Prof. Dr. ir. C. Lettieri,	Power and Propulsion Group TU Delft
	Assistant Prof. Dr. R. P. Dwight,	Aerodynamics Group, TU Delft

This thesis is confidential and cannot be made public until November 28, 2017.

An electronic version of this thesis is available at `http://repository.tudelft.nl/`.

TUDelft Delft University of Technology

PREFACE

Before you lies my Master of science dissertation titled "Numerical modelling of transcritical fluid behaviour using Lattice Boltzmann method", the motivation of which stems from my interest to add value to the literature and research on Supercritical Combustion in Gas Turbine Engines. A study results show that about 80% reduction in nitrous oxide emissions can be achieved by combusting the aircraft fuel at supercritical state. Thus this research direction has gained importance, due to which I undertook this project to exalt my career ambitions in the field of "Flight propulsion and Gas turbines".

This dissertation has been written to fulfill the graduation requirements of the Master of science program at the Faculty of Aerospace engineering, TU Delft. I was engaged in researching and writing this dissertation from May 2016 to December 2017. The research question was formulated together with my supervisor, C. Letteri. The results of this research effort is the development of a physics-based model to accurately capture trans-critical phenomena using Lattice Boltzmann methods, relevant to gas turbine applications. This research was challenging in adapting to new concepts and mathematically representing a physical phenomena with allowed assumptions. Nevertheless, I thoroughly enjoyed working on it with focus, as my thesis work adds to the body of knowledge to design low-emissions gas turbine engines.

I would like to thank my supervisor Dr. C. Letteri for guiding me with his expertise, time and apt support to have made this completion possible. He was available for my questions and crossroads throughout this phase to reach the final results.

I would also like to thank my parents and friends for their unconditional support and love. My parents and friends helped me with all they had to enable my best self and emerge successful with my graduation for which I am ever thankful.

I hope my dissertation is an interesting read for you as I have strived my best to make it one, until the last page.

S. Gunasekaran
Delft, November 2017

ABSTRACT

For the past fifty years, there has been a constant increase in the pressure ratio of gas turbines motivated by the need to increase the cycle efficiency. This has moved the operating pressure of gas turbine combustor to be above the critical pressure of jet fuels. This increasing trend in pressure of combustor, places the next generation gas turbines in supercritical regime of majority of jet fuels, making *Supercritical Combustion* a significant topic of research in the field of gas turbine. Understanding the fluid behavior at and above the critical point provides opportunity for better and efficient combustor design.

The complexity in numerical modelling of supercritical fluids, due to the dramatic property variations, solubility in gas and difficulty in tracking the vanishing interface, requires alternate modelling techniques that are well suited for treating multi-phase systems efficiently. Lattice Boltzmann Methods(LBM) is one such system gaining popularity in the recent decade due to the inherent capability to model complex multi-phase flows. LBM is a hybrid particle-continuum method based on the kinetic theory, which entails solution of the Boltzmann equation for the distribution function of particles properties on a lattice node.

Despite the advantages of LBM, there is considerable gap in effective application of this method as a solution for engineering problems. This research work is aimed to address this issue by creating a single and multi-component solver using LBM and making quantitative comparison with commercial fluid dynamic flow solver, ANSYS FLUENT. The results form created single-phase LBM solver agrees with the results from FLUENT single-phase solution in addition to showing superiority in terms of computational time and resources. In case of the multi-component model, LBM provided accurate results with coarser mesh refinement. A detailed investigation of LBM application for two simple systems has been studied and reported, thus laying a foundation for future numerical investigation of supercritical fluid modelling.

CONTENTS

LIST OF FIGURES

NOMENCLATURE

BC   Boundary condition

BGK   Bhatnagar-Gross-Krook

C – S   Carnahan-Starling

CFD   Computational fluid dynamics

CFL   Courant-Friedrichs-Lewy

EOS   Equation of State

FD   Finite difference

HCZ   He, Chen, and Zhang

LB   Lattice Boltzmann

LBE   Lattice Boltzmann Equation

LBGK   Lattice BGK

LGA   Lattice gas automata

N – S   Navier-Stokes

P – R   Peng-Robinson

PDE   Partial differential equation

PDF   Particle distribution function

R – K   Redlich-Kwong

RHS   Right hand side

RKS   Redlich-Kwong Soave

SC   Shan & Chen

vdW   van der Waals

Greek Symbols

α Thermal diffusivity

β Thermal expansion coefficient

δt Time step

List of Symbols

ΔT Temperature difference

$\delta x, \delta y$ Lattice space constant

κ Coefficient in surface tension term

λ Mean free path

μ Dynamic viscosity

ν Kinematic viscosity

Ω Collision operator

ω Relaxation frequency

$\Pi_{\alpha\beta}$ Momentum flux tensor

ψ Effective mass

ρ Fluid Density

ρ_w Wall density

σ Coefficient of surface tension

τ Relaxation time

τ_T Relaxation time for temperature field

$\mathbf{F}$ Forcing in Lattice system

$\mathbf{u}, u, \mathbf{U}$ Fluid velocity

$\mathbf{u}^{eq}$ Equilibrium velocity

θ Contact angle

a, b Constants of vdw parameters

c_0 Constant in equation of state

c_s Speed of Sound in Lattice units

D Dimension of space in the Lattice System; Diameter of the droplet

$e_k; c$ Velocity vector in Lattice system

f_k, g_k Particle distribution function

$f_k^{(eq)}$ Equilibrium particle distribution function

g fluid-fluid interaction strength; fluid-solid interaction strength

$G(x, x')$ Green's function (related to the fluid-fluid interaction potential)

g_f Strength of fluid-fluid interaction

g_w Strength of fluid-solid interaction

$G_w(x, x')$ Green's function (related to the fluid-solid interaction potential)

k Thermal conductivity; wave number

L Length of the domain, characteristic length

Nu Nusselt number

p Pressure

p^* Non- ideal part of pressure

Pr Prandtl number

R	Gas constant; radius
Ra	Rayleigh number
Re	Reynolds number
T	Temperature
t	Time
t^*	Non-dimensional time
T_0	Reference temperature
U'	Characteristic velocity
w_k, W_k	Weighting coefficients
x, x'	Position

Subscripts

b	Boundary node
cr	Critical value of parameters
f	Fluid node
i	Initial value
int	Interparticle
k, i	Lattice direction
Lu	Lattice unit
P	Physical Units
T	parameters related to Thermal LBM
w	Wall node

Superscripts

(eq)	Denotes equilibrium properties
(neq)	Denotes non-equilibrium properties
$*$	Denotes non-dimensional variables
$-$	Denotes average values

<div style="text-align: right">

1

</div>

INTRODUCTION

Numerical modelling can be defined as the description of a physical system with the help of predefined mathematical formulation. This research work is aimed at modelling behaviour of fluid from sub-critical to near critical and supercritical point (transcritical regime) using the Lattice Bolztmann Methodology. This introduction chapter discusses in detail about the background and relevance of the current thesis work. Section 1.1 outlines the need for research in supercritical combustion in gas turbines. Section 1.2 gives a brief description of the physics behind supercritical fluids, outlining the potential benefits of combustion taking place at supercritical conditions. Section 1.3 explains the complexity in modelling fluids and states the gap in knowledge for trans-critical fluid modelling. Section 1.4 provides the motivation for the use Lattice Boltzmann Method for numerical modelling. The scope and objective of this thesis is reported in Section 1.5 and Section 1.6 shows the related research questions. Finally, Section 1.7 provides the technical road-map of the research work.

1.1. MOTIVATION AND BACKGROUND

The global energy consumption predominantly depends on non-renewable energy resources, out of which natural gas and liquid fuel accounts for 23% and 33% respectively [1]. The increasing restrictions on emissions and the trend of the energy security resulted in the energy sector favouring towards liquid fired engines [2]. Hence, understanding the fluid behaviour at conditions prevailing in the combustion chamber of modern gas turbines is of great importance.
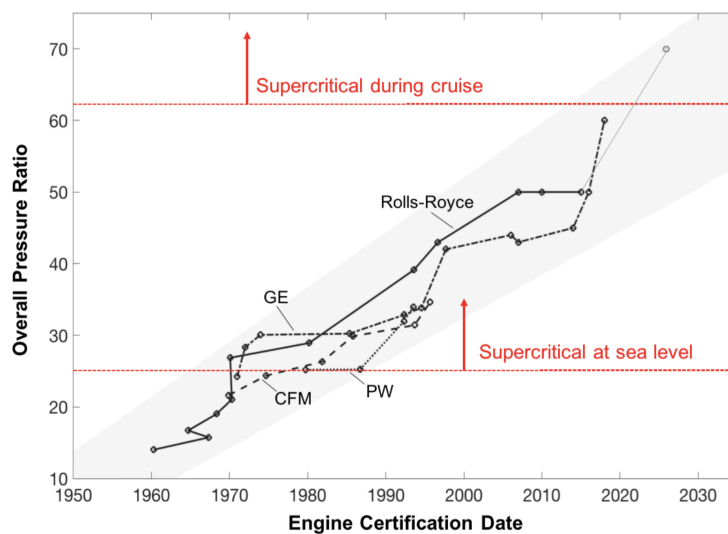
Figure 1.1: Gas turbine engine pressure ratio trend [3]

<div style="text-align: center">

1

</div>

Data from literature's [4] [5] [6] is represented in Figure 1.1 which indicates an increasing trend in the pressure ratios of typical aircraft engines motivated by the need for increasing the engine cycle efficiency. This results in the combustor pressure reaching near critical and supercritical regime for majority of the commonly used aircraft fuels. Figure 1.1 also predicts the pressure ratio to increase further in the future years suggesting that **Supercritical Combustion** will be an important topic of research in the field of gas turbine engines.
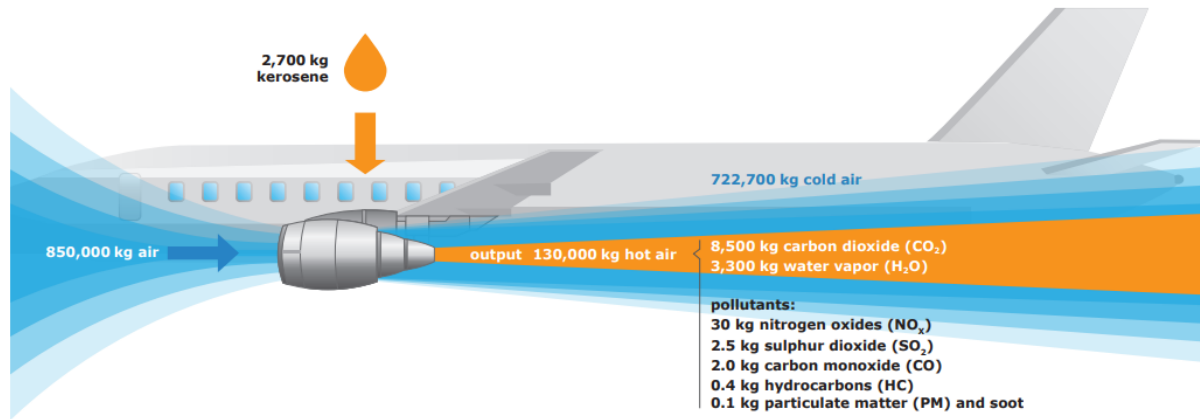
Figure 1.2: Emissions of a twin jet engine aircraft flying with 150 passengers for an hour [7]

A typical twin jet engine aircraft operating with 150 passengers for an hour produces $30\,kg$ of NO_x pollutants along with other emissions as depicted in Figure 1.2. Though the percentage of NO_x emissions is small (0.3%) compared to the CO_2 emission, its impact is highly toxic. NO_x emission at low altitudes leads to the formation of ground level ozone which might lead to serious health and climate problems that can accelerate global warming. The climate effects include acidification and eutrophication of water bodies and soil.
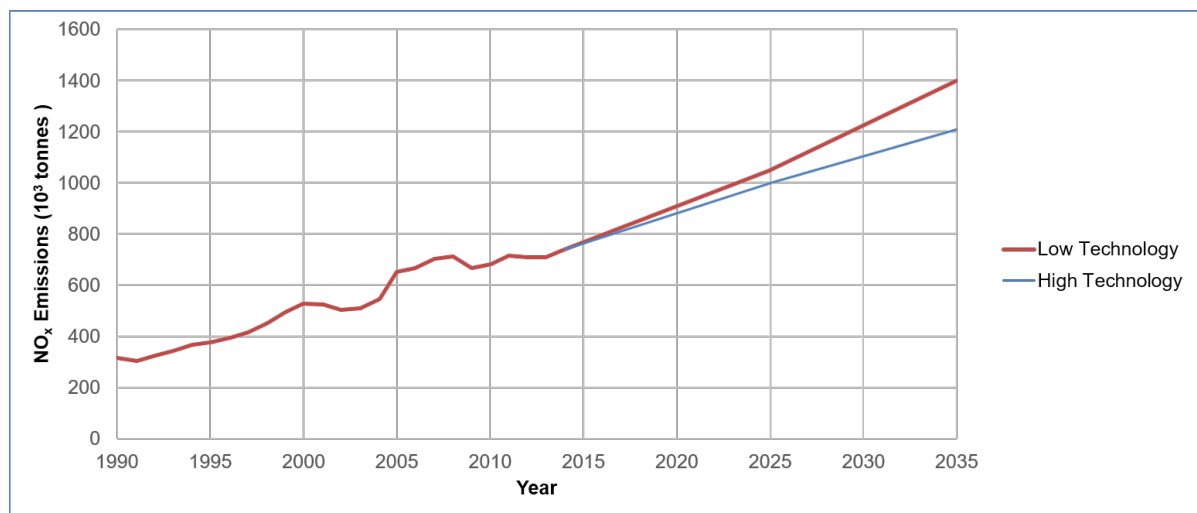
Figure 1.3: NO_x emissions trend from the European Aviation Environmental Report of 2016 [7]

The European Aviation Environmental Report [7], states out the history of NO_x emissions from 1990 till 2015, (Figure 1.3) along with a prediction for the next two decades by taking into account the anticipated increase in air-traffic and its impact in NO_x emissions. While looking into the historic data, the NO_x emissions in the year 2014 has been double the amount since the 1990's. The prediction of NO_x emissions has been done with two different cases, aircraft with the current engine technology (represented by the red line) and aircraft with advanced engine technology (represented by the blue line) at high air traffic scenario. The report suggests that there can be maximum of 14.2% reduction in NO_x emission with better and more sustainable aircraft engine technology.

In a typical gas turbine engine, the liquid fuel is introduced into the combustor through multiple injector holes during which the liquid fuel forms a film, breaks down into droplets, evaporates and mixes with the incoming air stream before combustion. During fuel-air mixing, the non-homogeneous mixture causes regions of large liquid fuel fragments near the vapour fuel which can lead to a high local flame temperature as shown in Figure 1.4. This in turn facilitates the formation of nitrogen oxides. From the Figure 1.4 it can also be seen that for the same flame temperature the liquid fuel also produces higher NO_x compared to the gaseous fuel. Non-uniform fuel-air mixture in a typical gas turbine results in increased formation of carbon monoxide (CO), nitrogen oxides(NO_x), hazardous air pollutants (HAP), volatile organic compounds (VOC) and particulate matter. Hence the major step to reduce the formation of nitrogen oxides would be enhance the mixing in combustion chamber. This can be done by moving the combustion process beyond the critical point of the liquid fuel. The physics behind supercritical fluid is briefly described in Section 1.2.
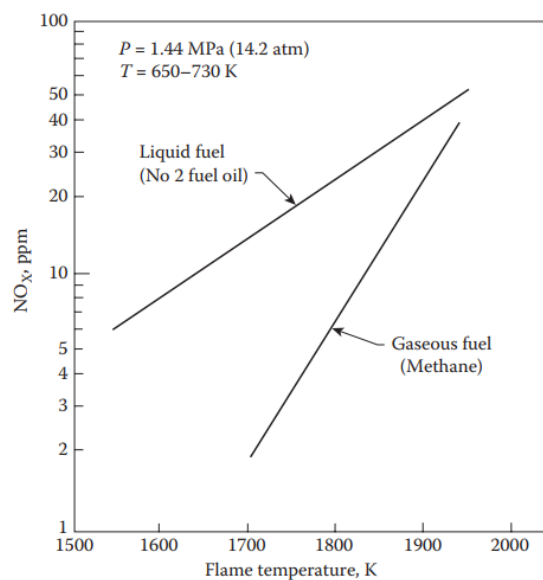
Figure 1.4: Dependence of NO_x on flame temperature for liquid and gaseous fuels[8]

1.2. PHYSICS OF SUPERCRITICAL FLUIDS

A fluid with temperature or pressure above the critical point is termed as a supercritical fluid. At supercritical conditions, the fluid undergoes dramatic variations with no phase change. When a fluid reaches the critical point the repulsive molecular forces become predominant overcoming the surface tension. Further pushing beyond the critical point, the sharp liquid fluid interface vanishes and a smooth density gradient is formed instead of traditional liquid breakup into droplets. At this point, the liquid fuel mixes with vapour fuel and air, to form a single phase fluid with liquid like density but with diffusive properties of gas. Figure 1.5 shows the fluid behaviour , when the fuel is injected in sub-critical and supercritical conditions. It can be observed that, at supercritical state there is no discrete droplets or sharp interfaces, but only a single phase fluid.
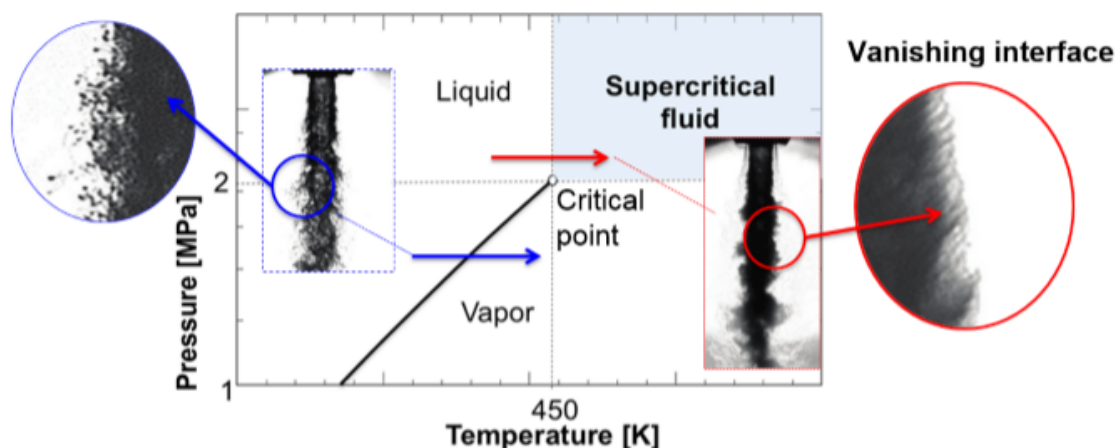
Figure 1.5: Injection of liquid fuel in subcritical (left) and supercritical (right) conditions [9]

The gas like diffusivity of supercritical fluid enhances the fuel-air mixing. This reduces the non-homogeneous mixture as a consequence of which formation of nitrogen oxide pollutants is reduced (as explained in Section 1.1). When the combustion takes place in supercritical regime, there can be up to 80% reduction in NO_x emissions as a result of enhanced fuel-air mixing [10] [11]. More detailed understanding of fluid behaviour near critical and supercritical regimes could provide opportunity for design of more sustained and efficient gas turbine combustors.

1.3. CHALLENGES IN TRANS-CRITICAL AND SUPERCRITICAL FLUID MODELLING

Due to dramatic variations in fluid properties at critical and supercritical regimes, there is an increased complexity in modelling. The selection of appropriate equation of state (as a result of deviation from ideal state) plays a vital role in the accuracy of the numerical model. When a fluid reaches the critical point, the density of gas and liquid phases becomes equal at the interface, but the magnitude of transport process remains the same across the fluid interface. The magnitude of transport processes and the timescales becomes same for both liquid and gas phase. This increases the difficulty in modelling as the gaseous phase transient effect cannot be neglected. For a fluid at supercritical state the there is increased diffusion due to the lack of intermolecular forces leading to solubility of the supercritical fluid into the surrounding medium. Along with the complex fluid behaviour issues, the vanishing surface tension at critical point provides a serious challenge in defining the phase front.

1.4. MOTIVATION TO USE LBM

Numerical modelling is a compelling tool to investigate and research chemical and physical systems for real engineering applications. There are two major approaches to computational modelling: continuum and discrete . The methods are selected based on accuracy and scale of the required simulation. Fluid flow in a typical gas turbine combustion chamber generally involves chemical reactions, heat transfer, fluid dynamics, multi-phase flows and phase change that occurs over scales ranging from macro-scale to micro-scale. Hence a brief overview of the two distinctive approaches is stated in the following sections including the necessity to use LBM.

1.4.1. CONTINUUM/MACROSCOPIC APPROACH

Continuum hypothesis is the approach adapted by most commonly available flow solvers. A fluid is made of numerous particles or molecules that move in random directions, within the system boundaries and colliding

with each other. The path that a particle travels in between collision with neighbouring molecules is termed as mean free path(λ). Assumption of continuum is valid for a fluid system with characteristic length scale greater than mean free path of the fluid ($L >> \lambda$). In other words, the state of an individual molecule does not affect the macroscopic property of the system. The continuum approach defines the system to be made up of multiple fluid elements, each representing a large number of molecules. The system is modelled with the help of ordinary partial differential equations based on Navier strokes equation to ensure the conservation of mass, momentum and energy. To deal with the complexity involved in solving the differential equations, the governing equations are discretized followed by initialisation and the solved interatively till convergence is achieved. One of the popular continuum based model is Reynolds Averaged Navier Strokes (RANS) in which the whole turbulence specture is modelled to reduce the computational time and resources. With advancement in computational power of the machines, more accurated models such as Large Eddy simulation (LES) and Direct Numerical Simulation (DNS) were formulated. These models provided results with more accuracy when compared with the RANS but came with the penalty of increased computational cost. Figure 1.6 shows how the accuracy of different numerical methods relates to the computational cost. The extent of modelling and assumptions associated with each of these continuum techniques are also represented in Figure 1.6. The major take away here is that, in continuum approach, the unnecessary information is neglected or modelled based on assumptions.

This does not affect the modelling or simulation of large scale problems such as, modelling flow over an airfoil. The inaccuracy arises in case of multi-fluid or multi-phase systems where the NS equation neglects the behaviour of individual molecules which actually defines the fluid interface by using non-bonded molecular interaction (long-range). The continuum approach will not be able to track multiple interfaces in such complex flows [12] [13].
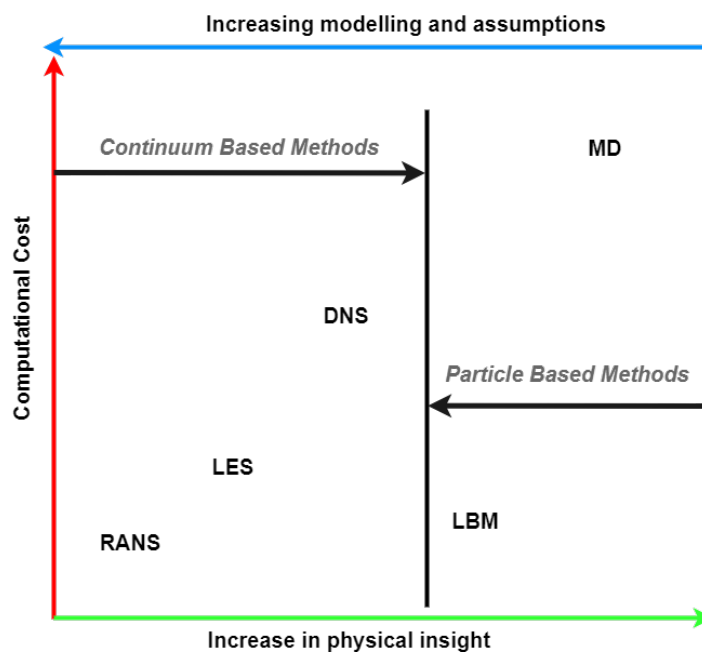
Figure 1.6: A hierarchy of modelling and simulation approaches based on [14]

1.4.2. MOLECULAR DYNAMICS/MICROSCOPIC APPROACH

The next type of numerical modelling based on discrete approach is called Molecular dynamics. This is a particle based simulation technique suited for micro-scale problems. Molecular dynamics tracks the location and velocity of each individual particle at every time step in order to simulate the fluid flow (see Figure 1.7). The macroscopic property of the system is dependent on the property of individual molecules. The estimation of the new position and velocity is based on Newton's second law of motion. Molecular dynamics can handle complex multi-phase and multi-fluid systems without additional forcing for tracking the interface, but the major draw back of this technique is the large amount of computational resources making the

approach unfeasible for real engineering application. To give an example, a volume of $1m^3$ of air contains approximately 2.5×10^{25} molecules at sea level. It can be concluded that with the current level of computational resources, it is impossible to solve large scale (magnitude of cubic *cm*) problems with molecular dynamics. Statistical mechanics serves as a bridge to connect the molecular information to the macroscopic information [12] [13].

1.4.3. LATTICE BOLTZMANN METHOD / MESOSCOPIC APPROACH

The challenges associated with continuum approaches to accurately capture the molecular behaviour and the impractical computational cost of molecular dynamics lead to the need of a new statistical method. This method is positioned at the centre of the hierarchy of major numerical modelling methods (as shown in Figure 1.6). Lattice Boltzmann method is a hybrid particle-continuum scheme. LBM defines the fluid to be made up of fictitious matter discretised in a structured lattice formation as shown in Figure 1.7. Instead of defining the property of each molecule, the LBM defines a collection of particles as a single unit located in each lattice node or space through a Particle Distribution function(PDF).

In accordance with classical mechanics, the LBM has two distinct steps streaming and collision for each lattice space, representing the molecule motion and collision. The distribution function when averaged over a long range gives the macroscopic property at each location in the lattice structure of the fluid.

Since the macroscopic properties are based on the distribution function on each lattice node, the fundamental behaviour of the set of particles, determines the fluid behaviour at the same time with less computational resources due to the grouping of molecules of similar property together. More detailed information of the same will be given in Chapter 2.

| Microscopic Approach | Statistical Approach | Continuum Approach |
| Newtons Equation | Boltzmann Equation | Navier Strokes Equation |

Increase in accuracy
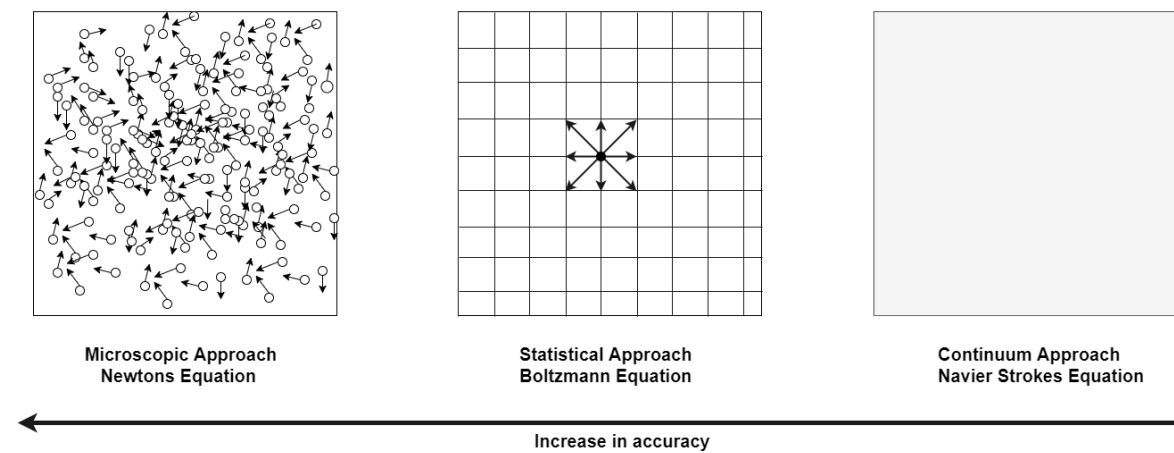
Figure 1.7: System definition in micro, meso and macroscale approach

In addition to this, in the case of multi-phase or a multi-component system, the interface can be easily defined by the forcing scheme and particle-particle collision with out assumptions or averaging the fluid in a particular grid. And one of the major difficulties in numerical modelling is definition of boundary condition which can be done with reduced complexity in LBM, which is explained in detail in Chapter 2, Section 2.8.

In Figure 1.7 the left most box represents the definition of a fluid using MD. It can be seen that each molecule along with it's velocity direction and magnitude is discretely defined. The middle box represents the fluid discretization into a lattice structure. And the directional arrows represents the possible directions of particle streaming. The right most box represents the definition of fluid using continuum approach where the fluid is divided into nodes and each node will contain a large number of molecules.

1.5. SCOPE AND OBJECTIVE OF THESIS

Despite the explained advantage, LBM is just gaining popularity and still has a gap for effective use in engineering applications. There is no consistent comparison of LBM with commercial available tools to quantitatively estimate the accuracy and computational cost. The complexity of creating a complete LBM solver for predefined single and multi-phase multi-component flows limited the extent of the current research work. This thesis will primarily be aimed at using LBM to create a single and multi-component solvers that can predict fluid dynamics and transport properties at sub-critical regime. Creating the LBM solver in sub-critical regime is the first step towards formulation of a supercritical LBM solver. In addition, the comparison of LBM's accuracy and computational cost with established numerical modelling tools will be reported.

Hence the major objectives of this thesis can be stated as follows:

- Create a single phase LBM solver for advection and thermal diffusion problems.

- Quantify the result of single phase LBM with existing solver-FLUENT.

- Create a robust multi-component LBM solver and compare the result with commercial tool (FLUENT).

- Create a thermal multi-component Lattice Boltzmann model.

1.6. MAJOR RESEARCH QUESTIONS

The research questions that guide this research work can be stated as follows:

- Can Lattice Boltzmann Method accurately predict transport properties of a multi-component system in sub-critical and near critical regime?

  - What can be inferred from comparing the newly developed multi-component LBM model with continuum-based fluid dynamic solvers?

- How computationally efficient is the single component lattice Boltzmann model when compared with the existing solver ?

1.7. TECHNICAL ROAD MAP

Figure 1.8 lays out the technical steps carried out to reach the goal of the thesis. First, a single component/phase system is modelled and simulated. The thermal and viscous boundary layer formed is compared and verified with results from FLUENT. This is carried out to ensure proper understanding and implementation of LBM. The next step involves creating the multi-component multi-phase LBM solver. The fluid dynamics of the model is verified with the case of a deformed droplet reaching steady state. In addition, the case of two droplets coalescing testcase is also considered. The final step consisted of incorporating thermodynamics into multi-component model simulating heat transfer between two fluids and verifying the results with FLUENT.
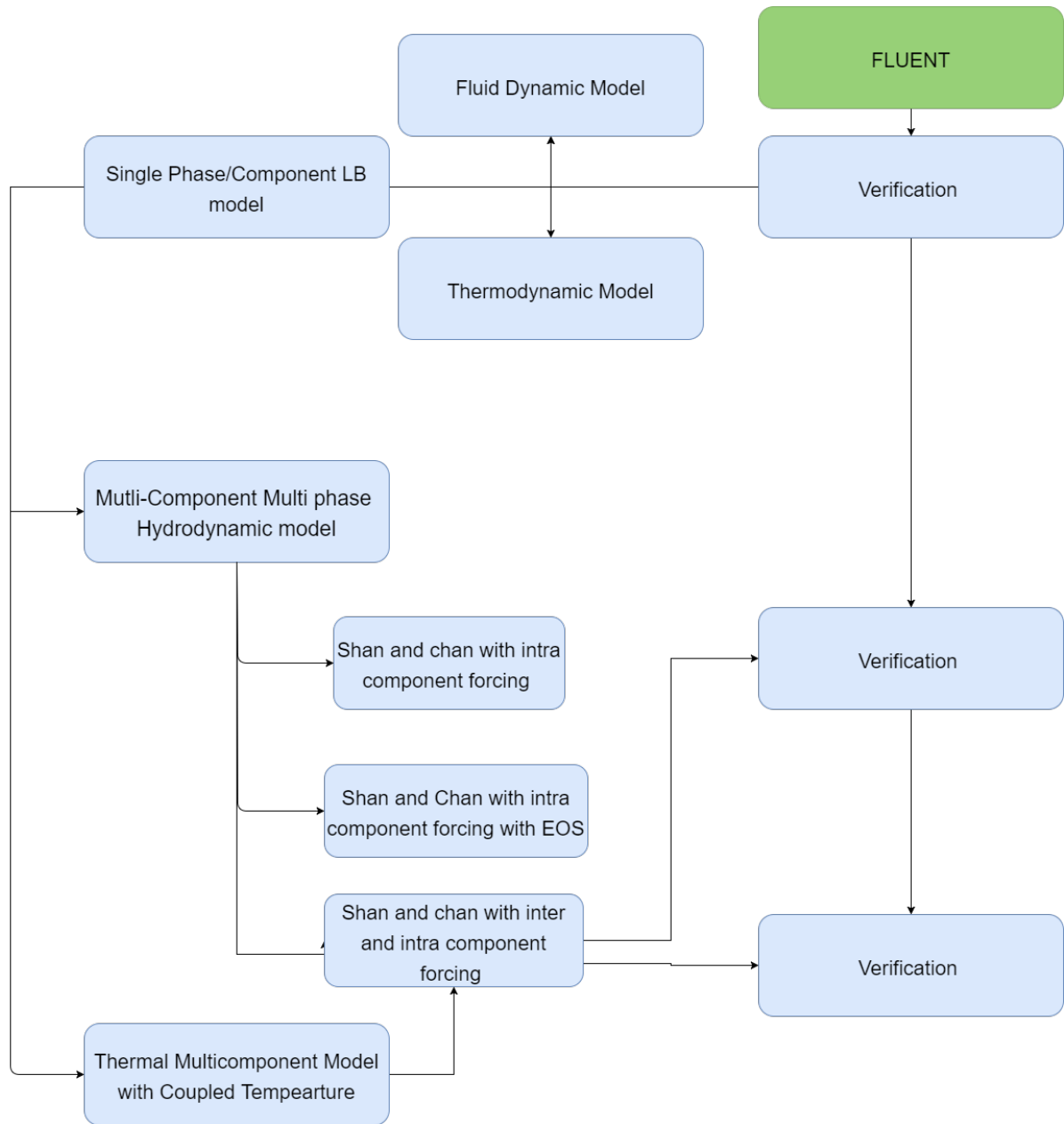
Figure 1.8: Technical Road Map of the Thesis

Figure 1.7 represents the thesis report structure. Chapter 2 explains the fundamentals of LBM, LBM units, viscous and thermal boundary conditions and relationship of the PDF with the macroscopic properties. Chapter 3 reports about the test cases considered for the verification of the fluid dynamics and thermodynamics of the single component LB model. Chapter 4 gives in detail about the fluid dynamics of multi-component model. It also outlines the forcing scheme selection and selection of interparticle strength that in turn defines the phase separation of immiscible fluids. The final part of Chapter 4 illustrates implementation of thermal model into the multi-component LB model. Chapter 5 describes the test cases for the verification of the fluid dynamics model followed by the case for thermal model. Chapter 5 also includes the comparison with FLU-ENT followed by a detailed description of all the observations. The conclusions are reflected in Chapter 6 together with the major contributions and recommendations for future work.
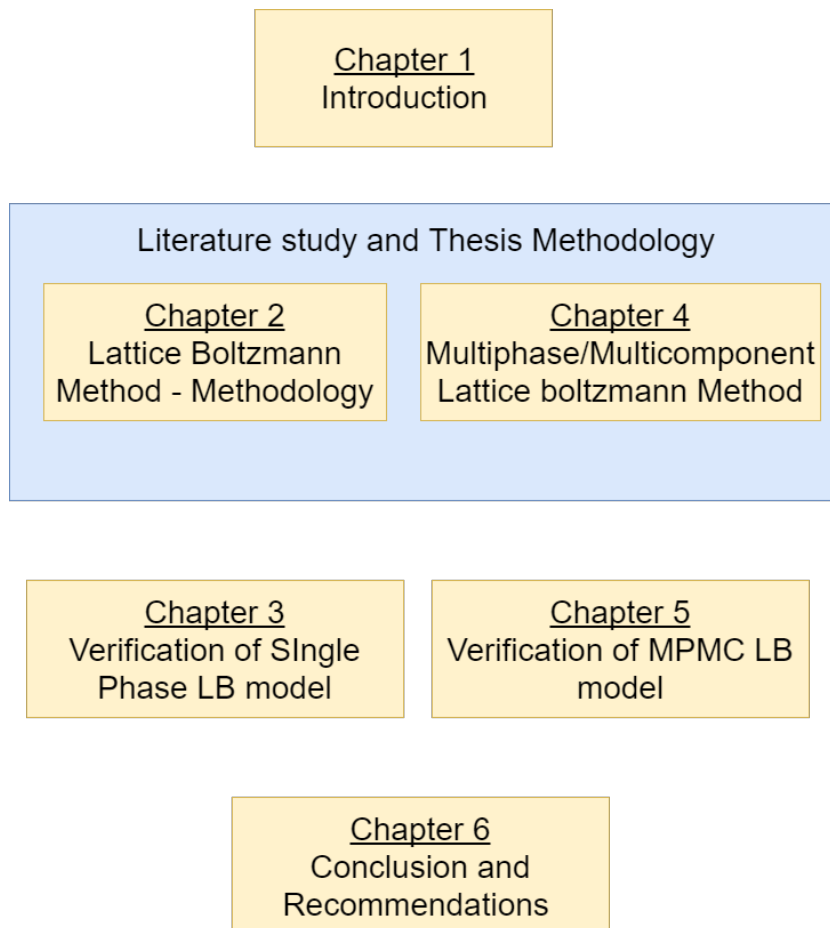
Figure 1.9: Thesis report structure

2

LATTICE BOLTZMANN METHOD

2.1. THE BOLTZMANN GAS CONCEPT

Ludwig Boltzmann was an Austria born scientist . His gas concept and the atomic theory of matter became very popular in the scientific community after his death. The basic concept of Lattice Boltzmann is that a gas is composed of large number particles whose interaction can be described by classical mechanics. Due to the large number of particles, an appropriate statistical treatment is needed. The study of classical mechanics is very simple and deals with streaming and collision interactions of particles [15] [16].

2.1.1. KINETIC THEORY

The simplified Boltzmann equation is derived from the kinetic theory of gases and statistical mechanics. The temperature and pressure are nothing but the magnitude of kinetic energy of molecules at the microscopic scale. When a force F is applied to a particle of mass m, the velocity and position of the particle changes. In absence of such a force, there is a free random movement of particles without change in direction and speed. When the system is heated, the kinetic energy of these particles on macroscopic level increases, which is termed as increase in temperature in the macroscopic world [15] [16].

The force exerted by the continuously bombarding particles per unit area of the walls of the container is a measure of pressure in macroscopic terms. Hence there is a relationship between pressure and temperature. When there is an increase in the kinetic energy of the particles due to the increase in temperature, the collision of the particles against the walls of the container increases resulting in increase in pressure[15] [16].

PRESSURE

According to Newtonian mechanics, the Kinetic Energy (KE) and pressure are related as follows,

$$P = \frac{2}{3} n \ KE \tag{2.1}$$

here n stands for the number of molecules per unit volume.

In a simple ideal gas model the molecular size and molecular interaction effects are neglected. The results of this model are valid for a gas at a room temperature but in a fluid near saturation, the particles have volume and the inter-molecular forces are no longer negligible [15] [16].

The ideal gas state equation is given as

$$PV = nRT \tag{2.2}$$

where, n denotes the of number of moles $n = \frac{N}{N_A}$, N_A is Avogadro's number and R is the gas constant [15].

From the above two equations 2.2 and 2.1, we can write

$$\frac{N}{N_A} \cdot RT = \frac{mc^2}{2}\left(\frac{2}{3}\right) \cdot N \tag{2.3}$$

Finally, now the Boltzmann's constant is introduced as ($k = \frac{R}{N_A} = 1.38 \times 10^{-23} J/K$), hence the kinetic energy of a gas is,

$$KE = \frac{mc^2}{2} = \left(\frac{3}{2}\right) \cdot KT \tag{2.4}$$

2.1.2. Boltzmann Transport Equation

The Lattice Boltzmann methodology predicts the properties of microscopic particles such as atoms and molecules determining physical properties such as thermal conductivity, viscosity and diffusion coefficient of macroscopic matter [15] [16].

In Boltzmann Methodology a fluid can be defined with the help of particle distribution function by adopting the statistical approach. The PDF f(x,c,t) represents the probability of finding molecules at specified location x and c at time t. Application of small force F displaces the position and velocity of the molecules to $x + cdt$ and $c + Fdt$ in the time interval dt. When the molecules represented by function $f(x,c,t)$ gets displaced to $f(x + cft, c + Fdt, t + dt)$, there is a possible collision of molecules. The collision results in change in the number of molecules due to the fact the final state might have molecules that did not initially start at x and some not arriving at $x + cdt$. Hence collision can be formulated as the rate of change of the PDF f [15] [16].

$$\frac{\partial f}{\partial t} = \Omega \tag{2.5}$$

The distribution function at an instance is dependent on x, c, t. After expanding the function f and simplifying, the Boltzmann transport equation can be written as the position and velocity vector for a particle after and before applying a force, F (see Equation 2.6)

$$\frac{\partial f}{\partial t} + \frac{\partial f}{\partial r} \cdot c + \frac{F}{m}\frac{\partial f}{\partial c} = \Omega \text{ [15]} \tag{2.6}$$

where, m is the mass of the molecules after collision process. The Boltzmann equation is solved by determining Ω (Ω is the Collision operator) which is a function of f. When there is no external force acting, the Boltzmann equation is formulated as Equation 2.7. The Equation 2.7 is an advection which can be easily solved along the characteristic line of tangent of the vector c if the source term Ω is know. The difficulty arises as the source term (Ω) is a function of f, with an integro-differential equation which is difficult to solve.

$$\frac{\partial f}{\partial t} + c \cdot \Delta f = \Omega \tag{2.7}$$

Here, c and Δf are vectors [15] [16].

2.2. The BGKW Approximation

A distribution function can be defined as the probability of finding the particles within a specific range of velocities, locations and at a given time. The Boltzmann equation is difficult to solve because the collision term yields complication. The collision operator can be approximated using the Maxwell-Boltzmann distribution without influencing the results of the simulation. This is because, the measured quantities are not significantly altered due to the collision of two bodies. Thus the BGKW (Bhatnagar, Gross, Krook and Welander) approximation was introduced for the collision operator which is a simplified model [15] [16].

The collision operator model is as below:

$$\Omega = \omega(f_{eq} - f) = \frac{1}{\tau}(f_{eq} - f) \tag{2.8}$$

where,

$$\omega = \frac{1}{\tau} \tag{2.9}$$

where the coefficient ω is the relaxation frequency and τ is the relaxation time.

The discrete Boltzmann equation along a specific direction can be written as

$$\frac{\partial f_i}{\partial t} + c_i \Delta f_i = \frac{1}{\tau}(f_i^{eq} - f i) \tag{2.10}$$

Some advantages of the above equation are:

- This is a linear partial differential equation.

- This equation represents an advection equation with the LHS consisting of an advection term (streaming process) and the RHS with a source term (collision process).

Replacing the tagging of each particle (as is the concept in Molecular dynamics) by the distribution function reduces the cost of computation.

2.3. UNITS AND LATTICE ARRANGEMENT

In the Lattice Boltzmann method,as the name suggests the solution domain is divided into lattices. The artificial particles (distribution function) reside at each lattice node. . The lattice arrangement decides the number of linkages and directions. These particles can stream to the nearby nodes along the directions defined by the lattice arrangement.

$DnQm$ refers to the dimension of the problem and the number of directional velocities. This is a common representation in LBM where n refers to the dimension of the problem (1 for 1-D, 2 for 2-D and 3 for 3-D) and m is the number of directional velocities and number of linkages. The commonly used lattice arrangement in this research the D2Q9 model. The Figure 2.1 represents a D2Q9 model where the $D2$ stands for two dimensional and $Q9$ stands for nine directional velocities.

The physical units and lattice units are related with the help of non-dimensional numbers. The reference [17] clearly details out the steps to be taken for the conversion. The physical units are converted to dimensionless quantities and then computed with the help of non-dimensional numbers such as Reynold's number and Prandtl's number which define the system. Basic physical units are converted to LBM units with the help of conversion factor. For instance a lenght of $4m$ in physical scale can be represented as $400lu$, then the conversion factor for length C_l can be calculated as follows

$$L_p = L_{lu} \times C_l \tag{2.11}$$

$$C_l = \frac{L_p}{L_l u} = \frac{4}{400} = 10^{-2} m \tag{2.12}$$

Similarly the basic units that define a system such as length(L), time(t) and denisty ρ are converted into lattice units.
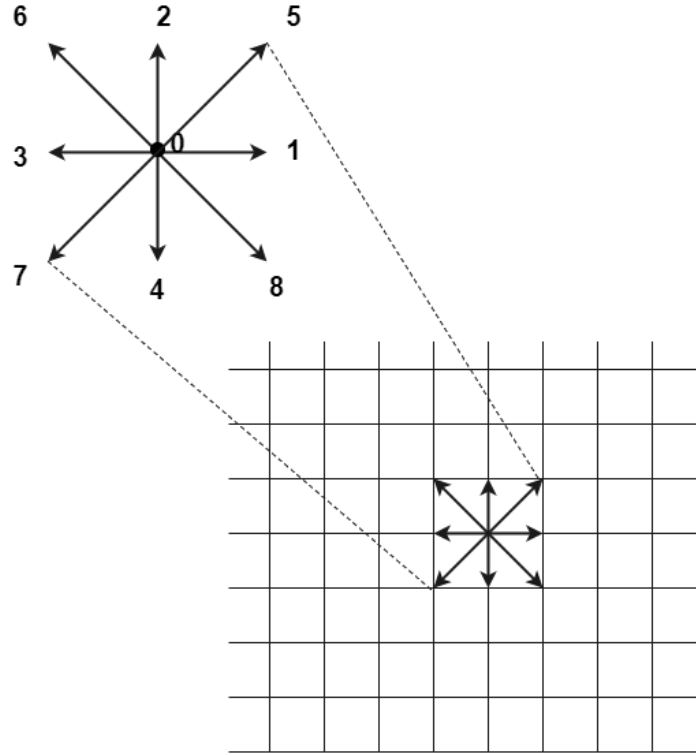
Figure 2.1: Simple D2Q9 LB model

2.4. Single relaxation time BGK

By applying the BGK (Bhatnagar-Gross-Krook) approximation to the collision term in a simple LBM equation, streaming and collision terms (i.e., relaxation towards local equilibrium) can be expressed as:

$$\underbrace{f_k(x + e_k \Delta t, t + \Delta t) = f_k(x, t)}_{\text{streaming}} - \underbrace{\frac{[f_k(x, t) - f_k^{eq}(x, t]}{\tau}}_{\text{Collision}} \tag{2.13}$$

where $f_a(x + e_a \Delta t, t + \Delta t) = f_a(x, t)$ is the streaming part and $\frac{[f_a(x,t) - f_a^{eq}(x,t]}{\tau}$ is the collision term, they represent the random motion and collision of molecules in LBM system. The term *Single relaxation time* indicates that the collision term is related to single relaxation time τ. τ is called the relaxation time which the set of molecules take to reach equilibrium after the collision. The relaxation parameter is integral while defining a system in LBM. It defines the thermal and viscous properties of a system and must be with in a specific value to maintain stability. The relationship between relaxation time and fluid property will be briefly explained in Section 2.5.

2.4.1. Macroscopic Variables

The macroscopic fluid density and velocity can be computed from the first and second order moment of the particle distribution functions[15] [16]. or PDFs (Refer Equations 2.14 and 2.15). The dimension and direction velocities are specified by the Lattice arrangements was explained in Section 2.3.

$$\rho = \sum_{a=0}^{8} f_k \tag{2.14}$$

$$\mathbf{u} = \frac{1}{\rho} \sum_{a=0}^{8} f_k e_k \tag{2.15}$$

2.4.2. Streaming

In streaming, the direction-specific densities f_k are moved to the nearest neighbour lattice nodes based on the corresponding velocity, this step is representation of motion of molecues in a fluid. The streaming scheme was originated due to Louis Colonna-Romano [16]. The Figure 2.2 illustrates the streaming process. The distribution functions corresponding to each directional velocity are computed at the beginning of the loops [15] [16]. From the Figure 2.2 it can also be noted that streaming does not alter the distribution function's magnitude (represented here by the length of the arrow) post streaming.
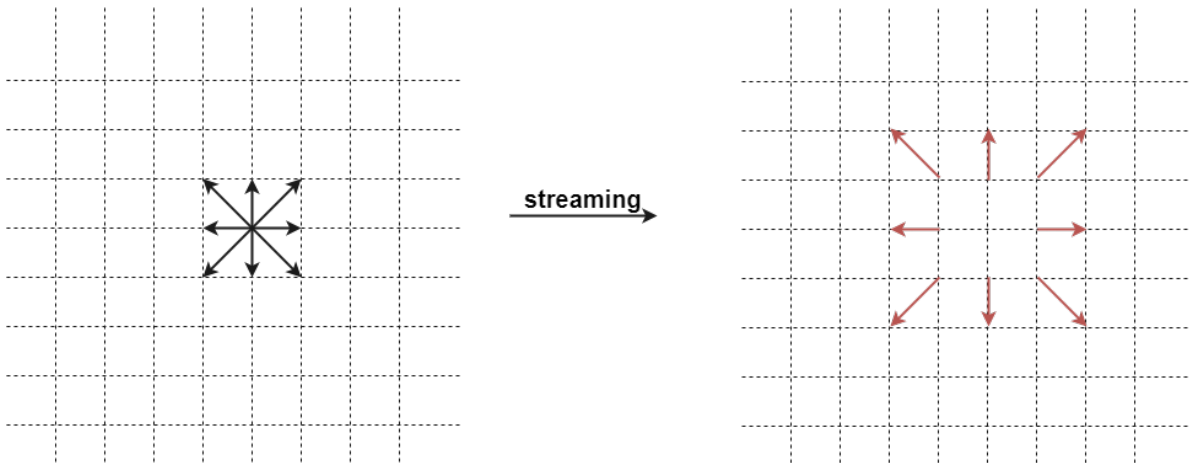
Figure 2.2: Illustration of the streaming process in **D2Q9** Lattice structure

2.4.3. Collision

The most important step of LBM is collision. The Equation 2.13 is a mathematical expression of the collision process. It averages out the PDFs before and after particle collisions. The pre and post collision PDFs along with their magnitude is shown in Figure 2.3
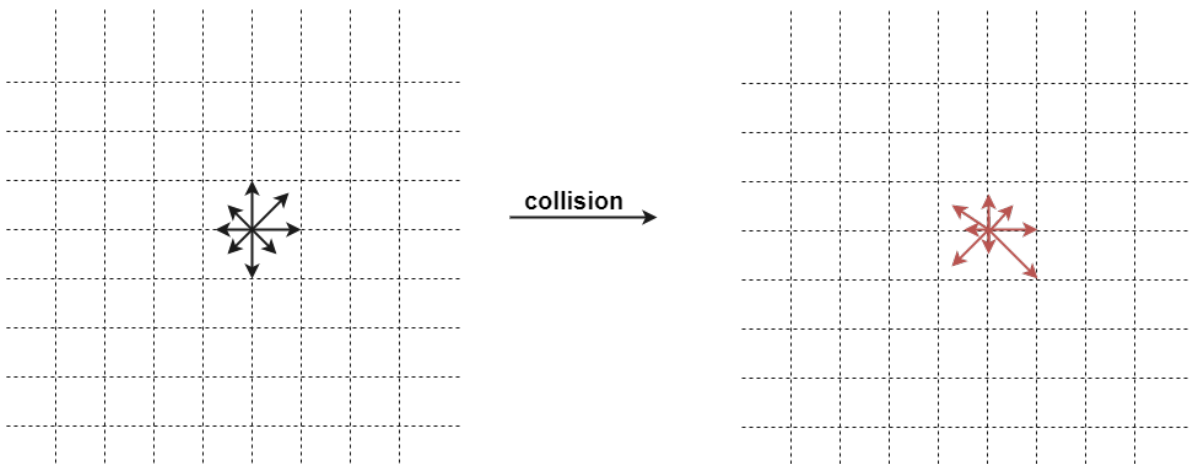

Figure 2.3: Illustration of collision process in **D2Q9** Lattice structure

It can be noted that after the collision, the magnitude of particle distribution functions changes with respect to the relaxation to the local Maxwellian rule.

2.4.4. EQUILIBRIUM DISTRIBUTION FUNCTION

The same LBM procedure can be used to solve different equations such as diffusion, advection–diffusion, momentum and energy equations with a variation in the equilibrium distribution function f^{eq}. Even different physical phenomena (such as for e.g, the wave propagation problem) can be solved using LBM methods but using the appropriate equilibrium distribution function [15] [16].

The normalised Maxwell's functions for particles of velocity u is given by Equation 2.16

$$f = \frac{\rho}{2\pi/3} e^{\frac{-3}{2}(c-u)^2} \tag{2.16}$$

The generalised form of the equilibrium distribution function formulated as in Equation 2.17.

$$f_k^{eq} = \Phi w_k [A + B c_k \cdot u + C(c_k \cdot u)^2 + D u^2] \tag{2.17}$$

where u is the velocity of the macroscopic particles. The constants represented by A,B,C,D can be determined based on conservation of mass, momentum and energy principles. Φ represents a scalar quantity such as density ρ for diffusion or temperature T (for conduction or convection problems) [15] [16]. The equilibrium distribution function for a flow with density ρ and velocity u obtained from the local Maxwell-Boltzmann equation, ignoring the higher order terms is given in Equation 2.18.

$$f_k{}^{eq} = w_k \rho \left[1 + 3 \frac{e_k \dot{u}}{c_s{}^2} + \frac{9}{2} \frac{(e_k \dot{u})^2}{c_s{}^4} - \frac{3}{2} \frac{u^2}{c_s{}^2} \right] \tag{2.18}$$

where e_k is the directional velocity based on the lattice structure in case of D2Q9, 9 possible velocity directions can be considered. w_k is the weights for each directional PDFs and for *D2Q9* model are

$$\begin{cases} w_{k=0} = \frac{4}{9} \\ w_{k=\{1..4\}} = \frac{1}{9} \\ w_{k=\{5..8\}} = \frac{1}{36} \end{cases} \tag{2.19}$$

where c_s is the speed of sound which is a lattice dependent quantity taking the value $c_s = \frac{1}{\sqrt{3}}$.

2.5. RELAXATION TIME AND FLUID PROPERTY

The relaxation time τ relates the fluid properties (such as Kinematic viscosity or thermal diffusivity) to the Lattice Boltzmann system. It can be computed from the Chapman Enskog Equation 3.7

$$\omega = \frac{\Delta t}{\tau} = \frac{1}{3\nu + \frac{1}{2}} \tag{2.20}$$

The above equation shows the relationship between kinematic viscosity and the relaxation time for density PDFs. For thermal PDF, the ν is replaced by α (Thermal diffusivity). Hence the relaxation time τ defines if the considered LBM system is hydrodynamic or thermodynamic. For stability issues literature suggests that τ should be within the values from 0.5 to 2.

2.6. STRUCTURE OF FLUID-DYNAMIC LBM SOLVER

The control flow of a simple LB method is represented in the Figure 2.4. The particle distribution functions are initialised with the help of the weightage factor w_i which is dependent on the lattice arrangements [15]. After the initialisation, the flow control enters the main loop which has collision and streaming for every iteration in a sequential order followed by application of appropriate boundary condition explained in Section 2.8. The macroscopic quantities can be computed as shown in Section 2.4.1.
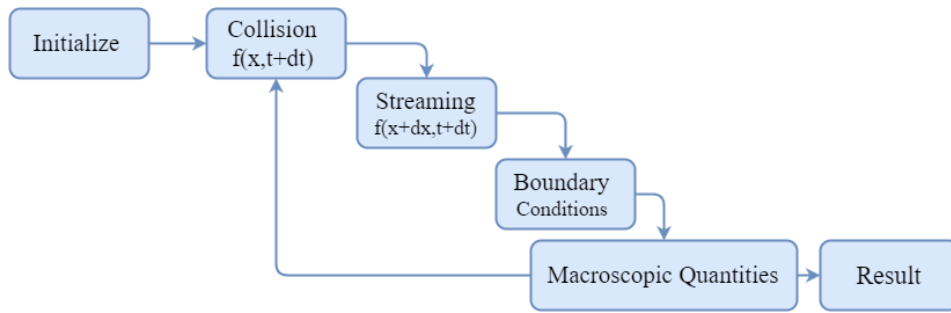
Figure 2.4: Control Flow of a Simple LBM

2.7. THERMAL LBM

The thermal LB method is similar to the Momentum LB method with the relaxation time τ_T is related to the thermal property, Thermal diffusion (α). The collision and streaming steps are carried out separately with a new set of PDFs related to the temperature of the system. Reynolds number and Prandlt number are used as the basis to derive the relaxation parameters for each PDF, making sure that the relaxation times (τ, τ_T) are representing the same system. The basic dependence chart for advection-convection flow is shown in Figure 2.5. It can noted that the velocity used in the equilibrium function of (g^{eq}) is derived from the second moment of the density distribution function (f). This indicates the one-way coupling of the thermal and momentum distribution functions making sure that the information about the boundary conditions such as no-slip will be transferred from the density to the thermal system.

$$g_k(x + \Delta x, t + \Delta t) = g_k(x, t)[1 - \omega_T] + \omega_T g_k^{eq}(x, t)$$
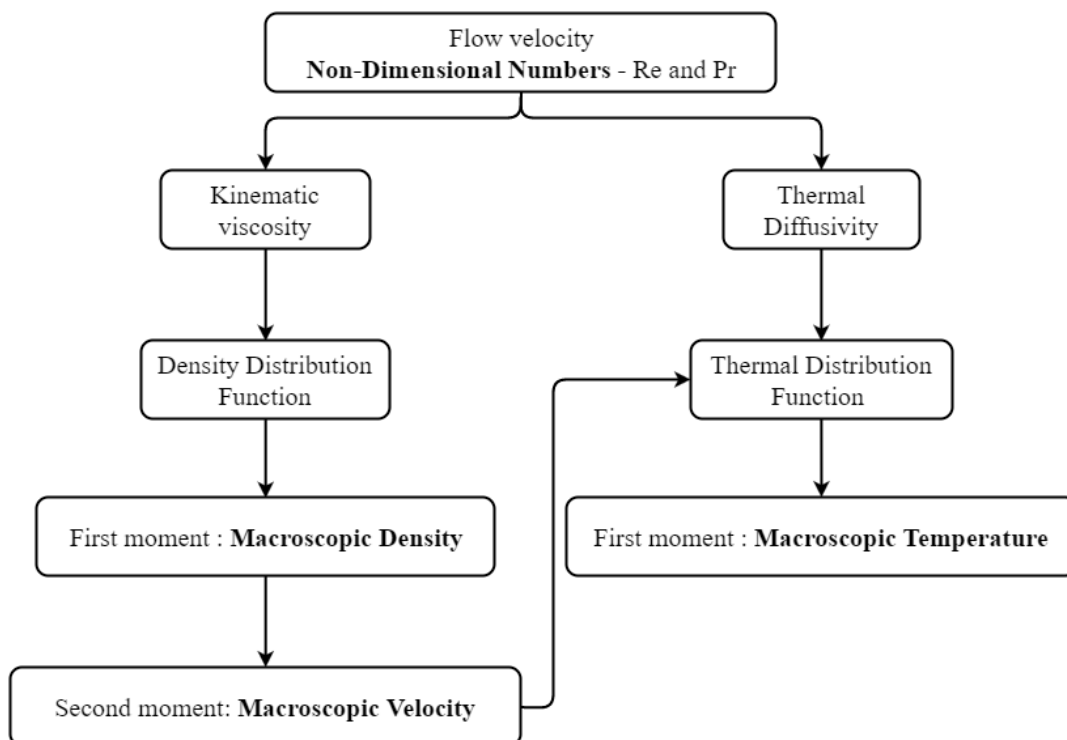(2.21)

Figure 2.5: Distribution function Dependence chart

2.8. BOUNDARY CONDITION (BC)

Boundary conditions forms one of the basics of any valid simulation. The flexibility in application of boundary conditions in LBM is highlighted as one of its major advantages [18] [15]. The major type of boundary condition based on the type of simulation can be broadly categorised into viscous and thermal. The single phase LBM solver created in this research work will have inflow, outflow and no-slip wall viscous boundary conditions and constant heat source thermal boundary condition. The implementation of the boundary condition is stated in the following subsections.

2.8.1. VISCOUS BOUNDARY

The no-slip boundary conditions are implemented by these Viscous BCs, also known as Bounce-back BCs. On reaching the boundary node, the fluid particle (represented by the discrete distribution function) will scatter back into the fluid along the same direction. There are two types of implementations of the Bounce-back BCs: The on-grid and the mid-grid bounce-back [18].

ON-GRID BOUNCE BACK BC

The on-grid bounce-back BC is known for it's simplicity. The lattice points are aligned with the fluid boundary in this configuration (see Figure 2.6). A boolean mask can be used for the interior and boundary nodes. The distribution function reverses its incoming direction when a boundary node is reached as showed in Figure 2.6. This configuration is well suited to simulate flow of fluid in complex geometries, for example, as in porous media flow or to indicate presence of solid body inside a flow [18].
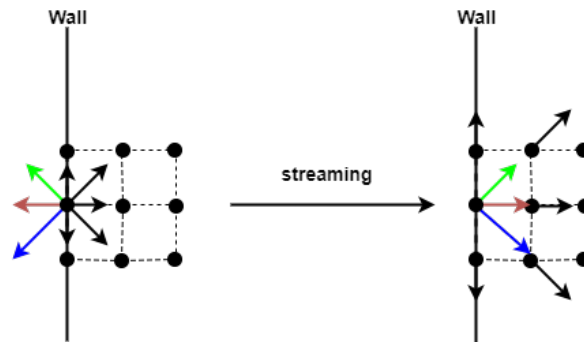

Figure 2.6: Illustration of on-grid bounce-back [18]

MID-GRID BOUNCE-BACK BC

The mid-grid bounce-back BC is a concept in which the boundary wall is placed between the boundary nodes of the fluid and the introduced fictious nodes as show in Figure 2.7.
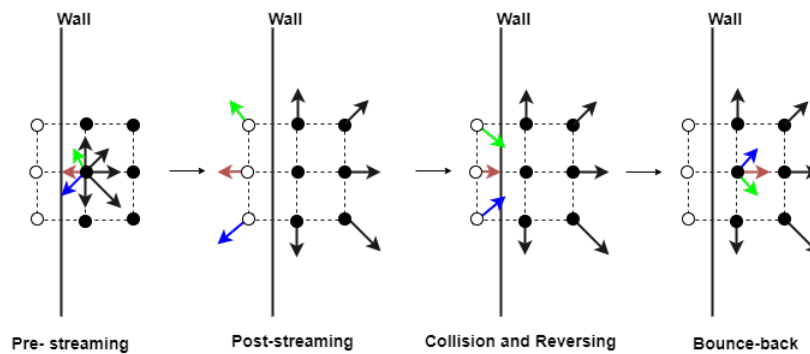

Figure 2.7: Illustration of mid-grid bounce-back [18]

All the distribution functions which are in the direction of the boundary wall would have left the domain at time step t. After this, the methodology of collision process is applied due to which the distribution function directions are reversed and they are bounced back to the boundary nodes. In the final bounce-back from the boundary nodes, the distribution functions are nothing but the post-collision distribution functions. The on-grid bounce back treats the streaming at the boundary in a one-sided way, and hence it leads to only a first-order accuracy despite it being easy to implement. The mid-grid bounce-back is modestly complicated to implement, but it results in a second order of accuracy due to its centred nature [18]. In this research work, on-grid bounce back is used for both the single and multi-phase multi-component LBM solvers

The inflow and outflow boundary conditions are implemented based on a methodology developed by Zuo and He, and is termed as the Zuo-He velocity condition. This boundary condition can be used in case of flows whose inlet and outlet velocity information is known. For instance, at the inlet the first node in the domain will be as shown in the Figure 2.8. Here the distribution functions 5,8,1 and density ρ at the inlet are unknown. Using the first order moment 2.22, x and y velocity components 2.23, 2.24 and equilibrium condition at the boundary 2.25 can be formulated.
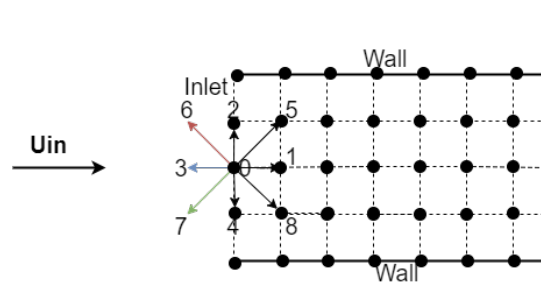

Figure 2.8: PDF at the inlet of a channel

$$\rho_{in} = f_0 + f_1 + f_2 + f_3 + f_4 + f_5 + f_6 + f_7 + f_8 \tag{2.22}$$

$$\rho_{in} u_x = f_1 + f_5 + f_8 - f_6 + f_3 + f_7 \tag{2.23}$$

$$\rho_{in} u_y = f_5 + f_2 + f_6 - f_7 - f_4 - f_8 \tag{2.24}$$

$$f_1 - f_1{}^{eq} = f_3 - f_3{}^{eq} \tag{2.25}$$

now we have four unknowns with four algebraic equations which can be easiy solved to get the values of ρ_{in}, f_1, f_5, f_8 [15]. The procedure is repeated for each lattice site in the outlet and inlet to find the boundary value of the unknown distribution functions and macroscopic parameter.

2.8.2. Thermal Boundary

Isothermal walls and constant heat flux walls are the two well known choices for the thermal wall boundary condition. Bao [19] provides descriptive steps on the derivation of the corresponding thermal boundary conditions.

When the isothermal wall is at a temperature T_w, the PDFs are unknown and they take the equilibrium distribution form as given in Equation 2.27, with an unknown temperature T'. The prescribed wall temperature can be used to determine the unknown temperature. As an example, the expression for the D2Q9 model at a lower boundary is given by the Equation 2.26:

$$T' = \frac{6}{1 + 3u_y + 3u_y{}^2} \left(T_w - g_0 - g_1 - g_3 - g_4 - g_7 - g_8 \right) \tag{2.26}$$

$$g_k^{(0)} = w_k T \left[1 + \eta_k \cdot \mathbf{u} + \frac{1}{2} (\eta_k \cdot \mathbf{u} \eta_k \cdot \mathbf{u})^2 - \frac{1}{2} u^2 \right] \tag{2.27}$$

where the summation of the equilibrium distributions has replaced the summation of the unknown PDFs i.e,
Now using T' in the equilibrium distribution equation gives the unknown PDFs.

<div align="right">

3

</div>

VERIFICATION OF SINGLE PHASE LATTICE BOLTZMANN MODEL

Chapter 2 gave a detailed description of the Single Component LBM. This chapter deals with the application of the LB methodology to a simple physical system with both thermal and viscous boundary conditions. Creation and verification of a single component LBM solver marks the application of LBM for single phase problems. This Chapter also reports the quantitative comparison of the newly formulated LBM solver with an existing commercial solver such as FLUENT.

3.1. PROBLEM SPECIFICATION

A 2-D channel for L/B ratio of 4 is considered, where L and B is the length and breadth of the channel. Cold air flows in the channel with uniform velocity of $0.00146 m/s$. The inlet temperature T_{in} of air is $293.15K$. The walls of the channel are kept at a constant temperature T_{wall} of $303K$. In a gas turbine combustor, the typical Reynolds number based on droplet diameter is in the order of 100 [20]. Hence for single component LBM test case, the flow Re is set as 100 and with the channel breadth of $1m$, the flow velocity is calculated to be $0.00146 m/s$.

From the transport properties, the Prandtl Number (Pr) is calculated to be 0.744. These two non-dimensional numbers enable the conversion of physical units into lattice units (lu). Figure 3.1 shows a representation of the problem. The simulation of this flow ensures the working and comparison of the created LBM single phase/component model with commercial tool in addition to verifying correct coupling of the thermal and momentum LBM models.
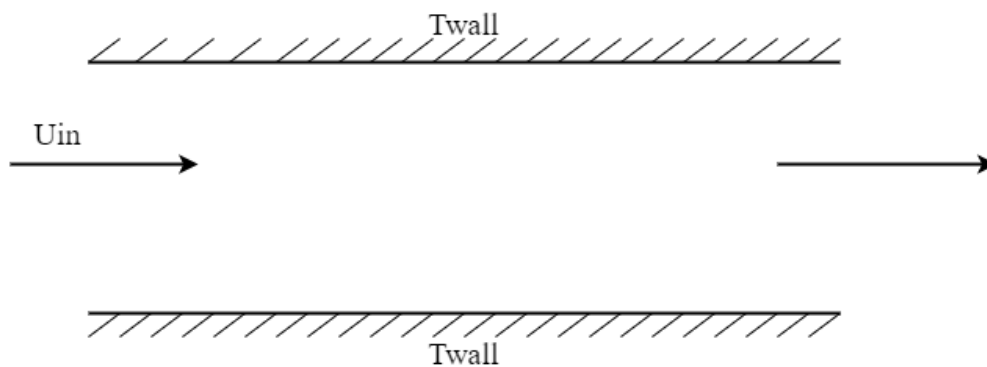

Figure 3.1: Domain configuration of 2D channel with cold air flow and heated walls

3.2. ASSUMPTIONS OF THE TEST CASE

Below are some assumptions that were made to simplify the problem under study:

- Uniform inlet velocity.

- Incompressible viscous flow.

- Two-dimensional channel.

3.3. LATTICE BOLTZMANN SYSTEM SPECIFICATIONS

The physical length of the tube is $4m$ which is discretized to 400 lattice nodes in the LB system. The mesh yields 100 cells in the direction orthogonal to the wall. The conversion factor for the length and time scales can be computed as follows:

$$L_p = L_{lu} \times C_l \tag{3.1}$$

$$Cl = \frac{L_p}{L_{lu}} = \frac{4}{400} = 1 \times 10^{-2} m \tag{3.2}$$

$$U_p = U_{lu} \times \frac{C_l}{C_t} \tag{3.3}$$

$$C_t = 0.146 \times \frac{10^{-2}}{0.00146} = 1s \tag{3.4}$$

The subscripts p and lu represent physical and lattice units respectively. The kinematic viscosity in lattice units is calculated as follows:

$$Re = \frac{U_p B_p}{\nu_p} = \frac{U_{lu} B_{lu}}{\nu_{lu}} = 100 \tag{3.5}$$

$$\nu_{lu} = U_{lu} \times \frac{B_{lu}}{Re} = 0.146 \times \frac{100}{100} = 0.146 \frac{lu^2}{lt} \tag{3.6}$$

The relaxation frequency ω is calculated from the kinematic viscosity (ν_{lu}) using the following formula derived from Chapman-Enskog expansion,

$$\omega = \frac{1}{3\nu_{lu} + \frac{1}{2}} = \frac{1}{3 \times 0.146 + 0.5} = 1.066 \tag{3.7}$$

The thermal lattice parameters can be derived from the momentum lattice parameters. The thermal relaxation frequency is related to the thermal diffusivity α. The thermal diffusivity and the kinematic viscosity of a system is related with the Prandtl number. Hence, the thermal diffusivity for the defined momentum system can be computed as follows:

$$Pr = \frac{\nu_p}{\alpha_p} = \frac{\nu_{lu}}{\alpha_{lu}} \tag{3.8}$$

$$\alpha_{lu} = \frac{\nu_{lu}}{Pr} = \frac{0.146}{0.744} = 0.196 \frac{lu^2}{lt} \tag{3.9}$$

Similarly, the relaxation frequency of the thermal LB model can be computed using the Equation 3.7, resulting in $\omega_t = 0.919$.

3.4. Single Component/Phase results Verification

The LBM simulation is run until the system reaches steady state. The velocity and thermal profile at different locations of the channel is compared with the simulation results in FLUENT. The locations are selected to be at 12.5% , 50% and 87.5% of the channel length, as show in Figure 3.2. These respective locations are selected so as to capture the parameters profile near the inlet, mid and outlet sections of the channel. Comparing the fluid properties along the channel lengths provide an opportunity to report the development of thermal and velocity boundary layers.
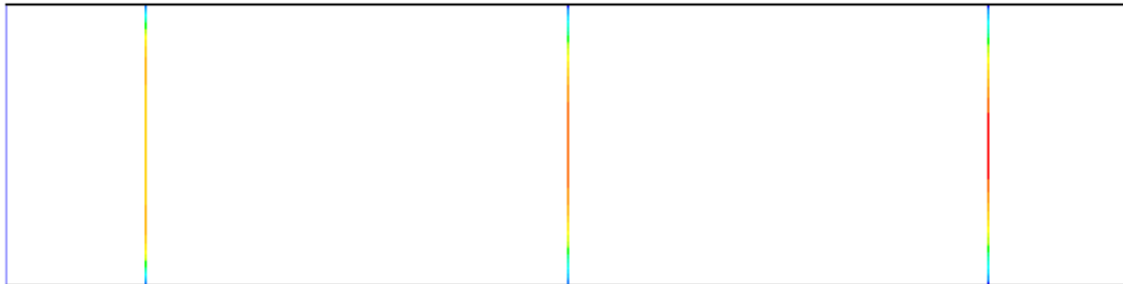
Figure 3.2: Channel domain with locations at which the fluid parameters are compared

In FLUENT, two mesh configurations are considered, where one is identical to the LBM mesh (Refer Figure 3.3), i.e. 400×100 cells and a mesh configuration with higher refined mesh 1600×400 such that the grid size near the walls is smaller than the boundary layer thickness so as to accurately capture the flow field (refer Figure 3.4). In addition to the mesh refinement, the FLUENT test case is run with all the four available solution schemes of Pressure-Velocity coupling.

Figure 3.3: Representation of a square mesh

Figure 3.4: Zoomed refined mesh near the channel wall

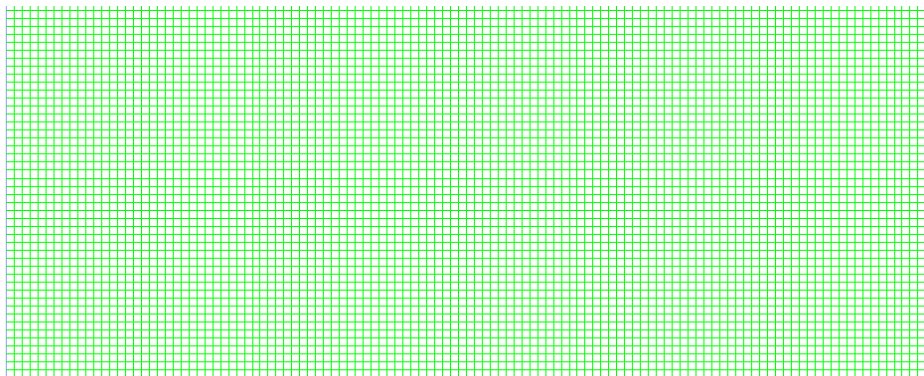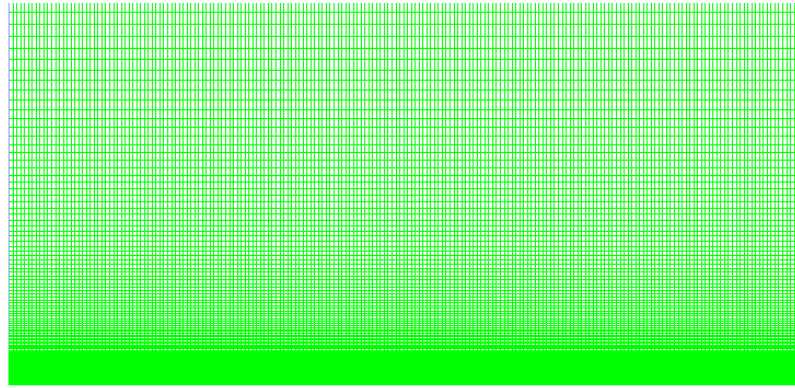A short description of the solution schemes available in FLUENT for Pressure-Velocity coupling are as follows:

- SIMPLE: In SIMPLE solution scheme, the pressure field is obtained by enforcing the conservation of mass with the help of pressure and velocity relationship [21].

- SIMPLEC: The second type of solution scheme available in FLUENT is SIMPLEC or SIMPLE-Consistent pressure velocity solution scheme, which is quite similar to the SIMPLE scheme with respect to the solution procedure. The only difference between the two schemes lies in the correction expression [21].

- PISO: Another variant of the SIMPLE algorithm in FLUENT is the Pressure-Implicit with Splitting of Operators (PISO). The PISO solution scheme is equipped with two additional corrections to improve the efficiency of the calculations. This is due to the fact that in case of the SIMPLE and SIMPLEC algorithms the momentum balance is not maintained with the new velocities and their respective fluxes, as a result the calculation is repeated until balance is reached. The presence of neighbour correction and skewness correction in PISO solution scheme increases the algorithm's efficiency [21].

- Coupled: Unlike segregated approaches where each equation while evaluation is decoupled from the other equations, this pressure based solver in FLUENT provides additional feature to solve the considered flow problem in a coupled manner. The coupled scheme solves the continuity, momentum , energy equation(in case of thermal boundary) and the species transport simultaneously by considering them as a set or vector of equations and the governing scalar equation will be segregated and solved sequentially . It provides a robust solution scheme for steady state single phase problems. In case of transient problems with poor mesh quality it is necessary to use coupled scheme. The coupling scheme also has an advantage of enabling the use of larger time step when compared with the other available solution schemes [21].

3.4.1. COMPARISON OF RESULTS

IDENTICAL MESH

Figures 3.5, 3.6 and 3.7 show the velocity profiles at the selected locations for the identical meshes. Each plot contains the velocity profile obtained from all the four available solution schemes in FLUENT along with the result from LBM solver. Figures 3.8, 3.9 and 3.10 show the temperature profiles at 12.5%, 50% and 87.5% of the channel locations.
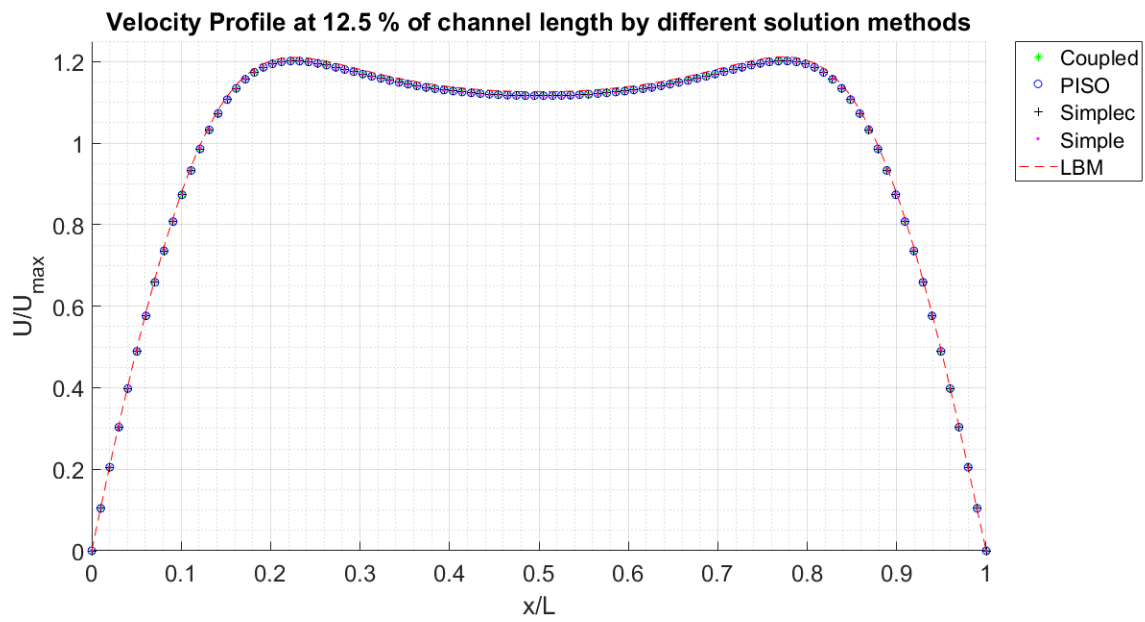
Figure 3.5: Velocity profile comparison at 12.5% of the channel length
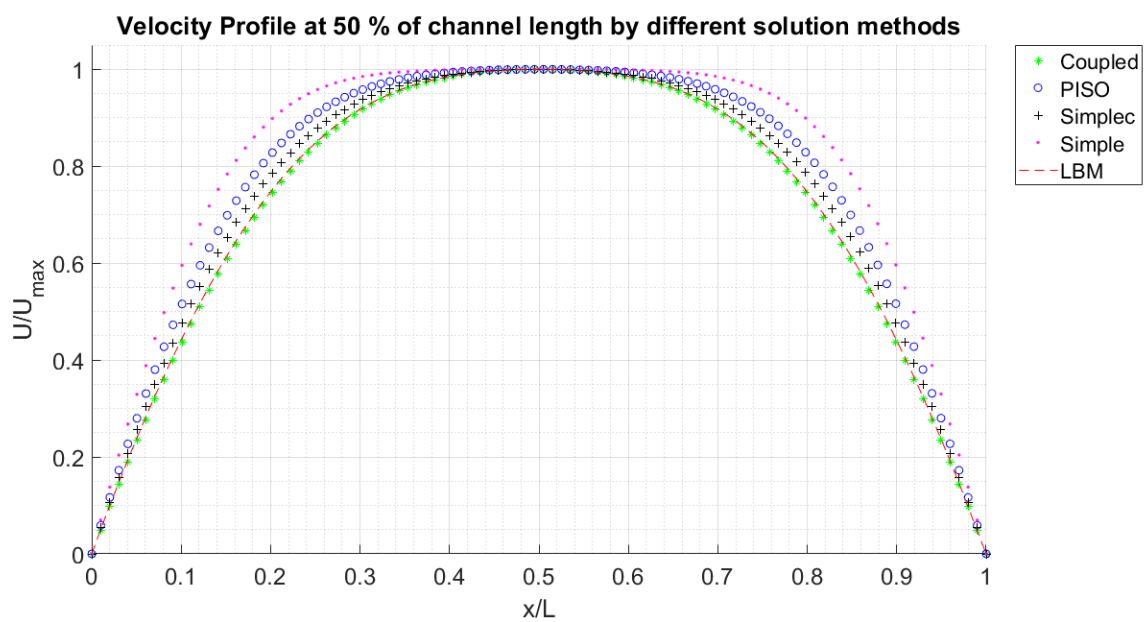

Figure 3.6: Velocity profile comparison at 50% of the channel length
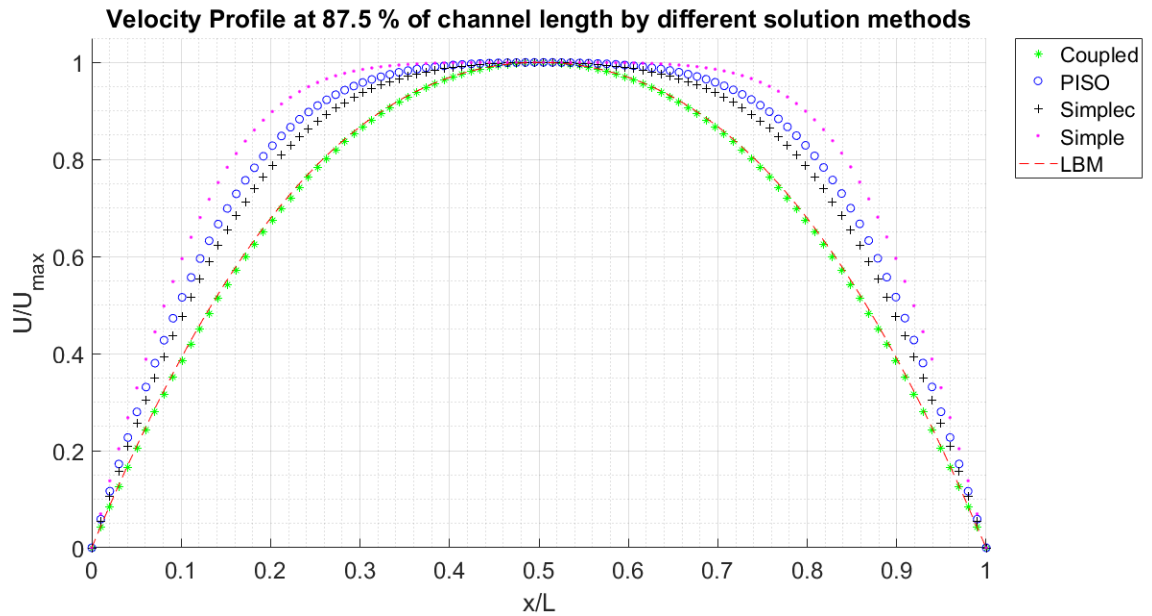
Figure 3.7: Velocity profile comparison at 87.5% of the channel length

The velocity profiles at different sections show the development of flow along the channel length. A fully developed flow is expected to have a parabolic shape which can be seen in the results from the LBM solver and Coupled solution scheme of FLUENT (see Figure 3.7). The velocity profiles obtained from SIMPLE, SIMPLEC and PISO show a velocity profile that is not fully developed even at 87.5% of the channel length. This is due to the fact that the velocity boundary layer is not accurately captured near the walls due to reduced mesh refinement. The SIMPLE scheme shows a deviation of more than 19% from the COUPLED scheme and LBM results. Where as the LBM results are in good agreement with the result obtained from COUPLED scheme of solution method with a percentage difference in the order of 0.902%. PISO and SIMPLEC schemes have a percentage difference of 14% and 10.54% respectively from the LBM results .

Figure 3.8: Temperature profile comparison at 12.5% of the channel length

Figure 3.9: Temperature profile comparison at 50% of the channel length

Figure 3.10: Temperature profile comparison at 87.5% of the channel length

Normalised temperature T_n is computed as shown in Equation 3.10. Figures 3.8, 3.9 and 3.10 show the temperature profile obtained from the identical mesh. It can be stated that there is good agreement of results between the methods considered. The maximum deviation between the LBM and FLUENT results is less than 1% in case of coupled solution scheme.

$$T_n = \frac{T - T_{cold}}{T_{hot} - T_{cold}} \tag{3.10}$$

where T_{cold} and T_{hot} is the minimum and maximum temperature of the system.

As already stated in Section 3.4 the simulation is run with a mesh four times more refined (1600×400) than the mesh used in the LBM solver. Local refinement near the walls assumed to capture the velocity and thermal boundary layer accurately. The thermal and velocity profiles at the selected locations of the channel length can be seen in Figures 3.14, 3.15, 3.16, 3.11, 3.12 and 3.13 respectively.

Velocity Profile at 12.5 % of channel length by different solution methods

Figure 3.11: Velocity profile comparison at 12.5% of the channel length

Velocity Profile at 50 % of channel length by different solution methods

Figure 3.12: Velocity profile comparison at 50% of the channel length
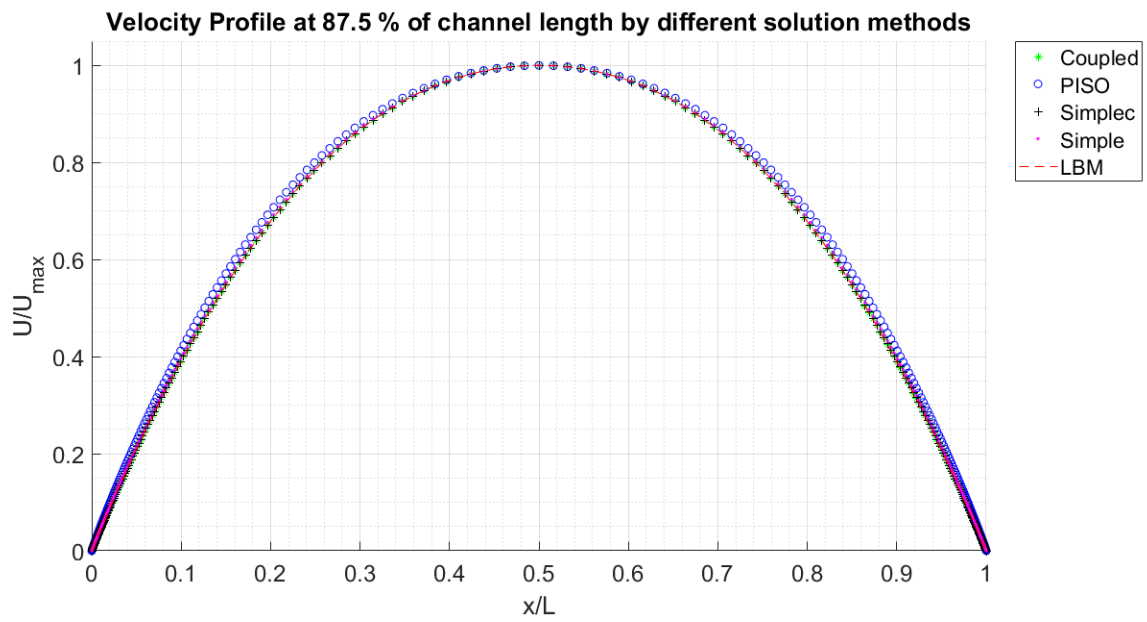
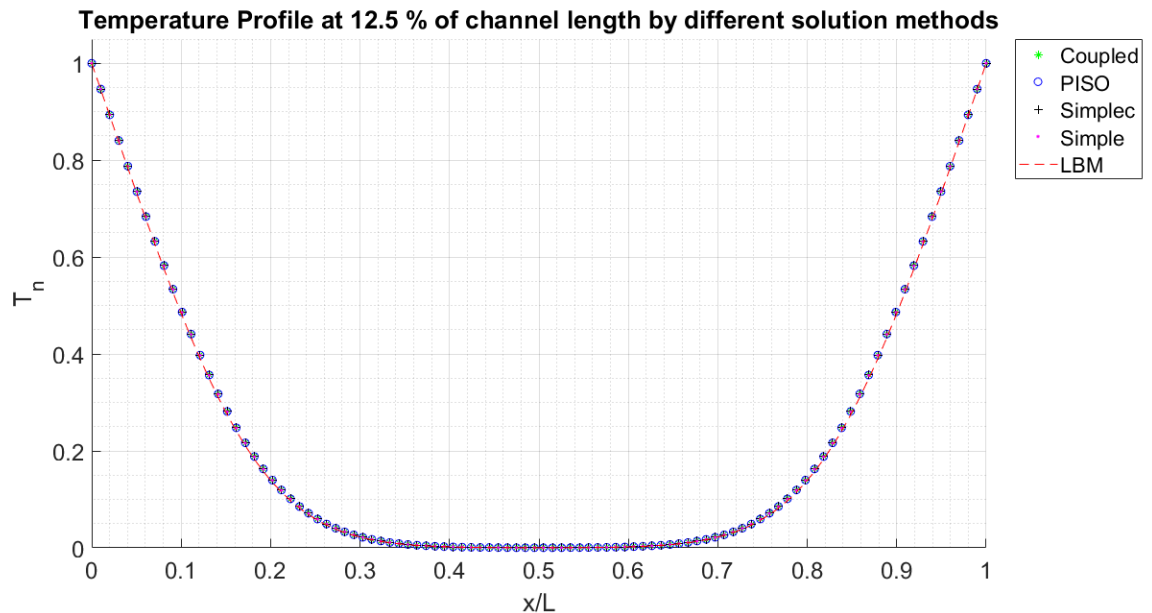Figure 3.13: Velocity profile comparison at 87.5% of the channel length
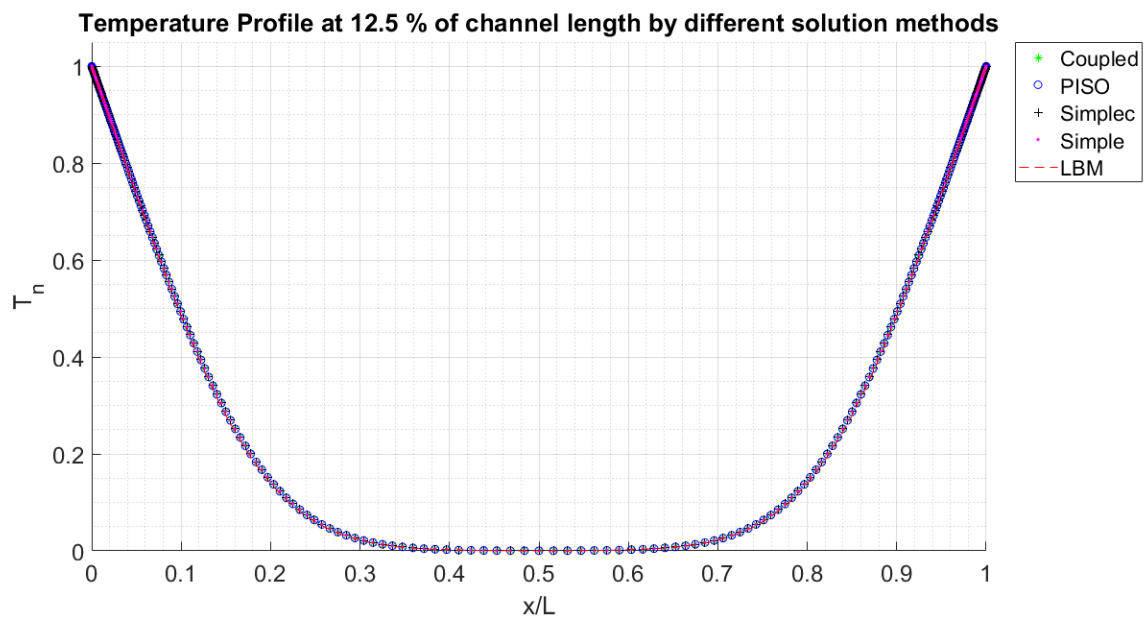
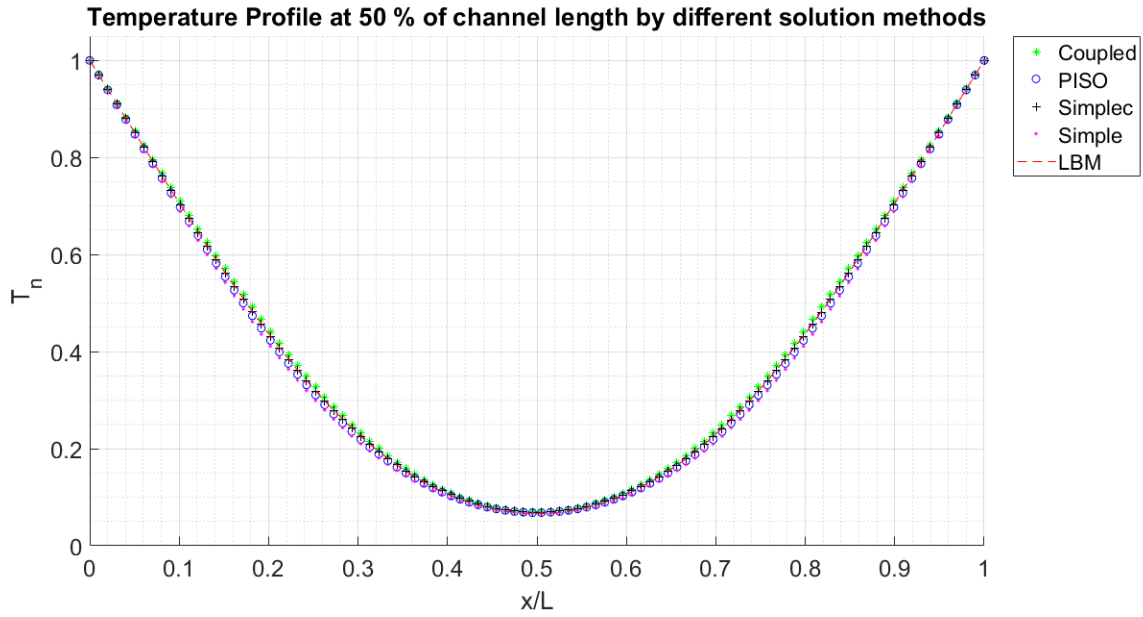Figure 3.14: Temperature profile comparison at 12.5% of the channel length

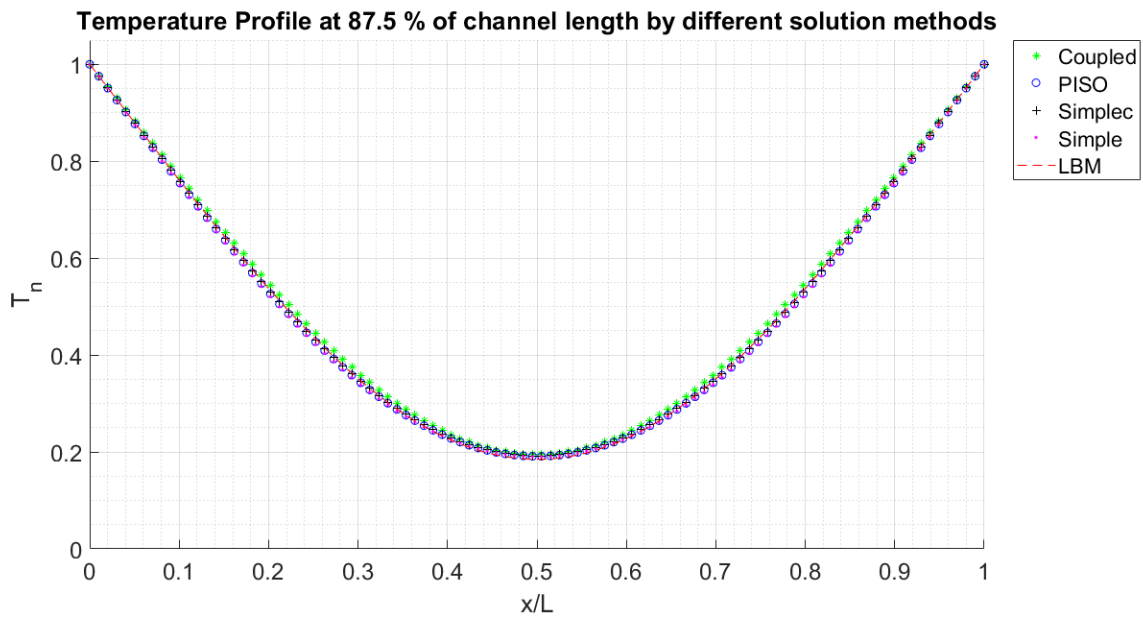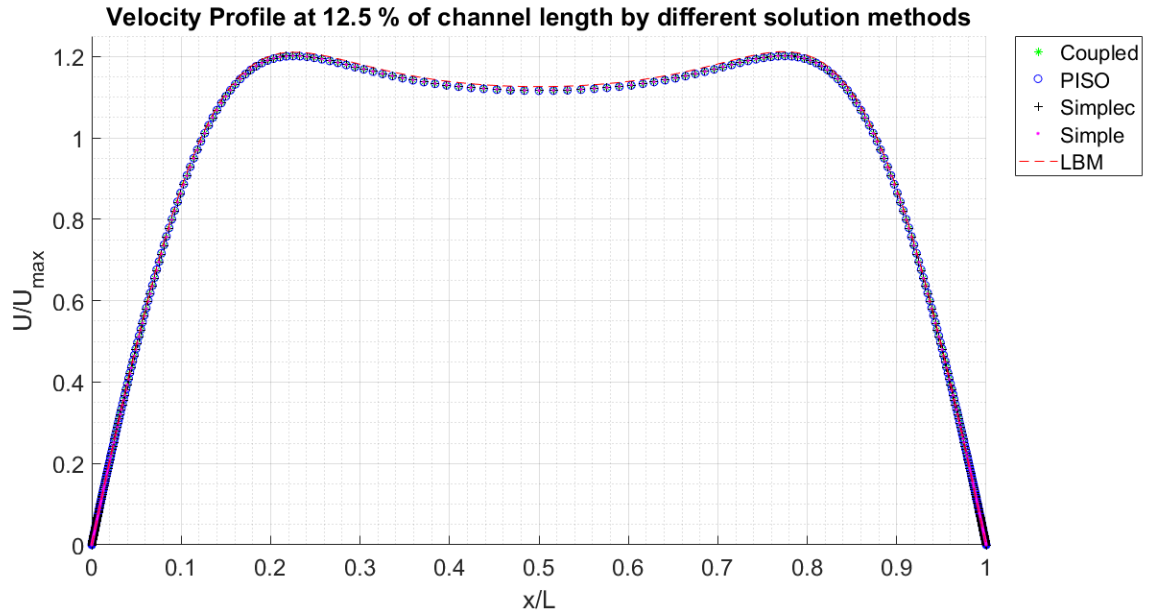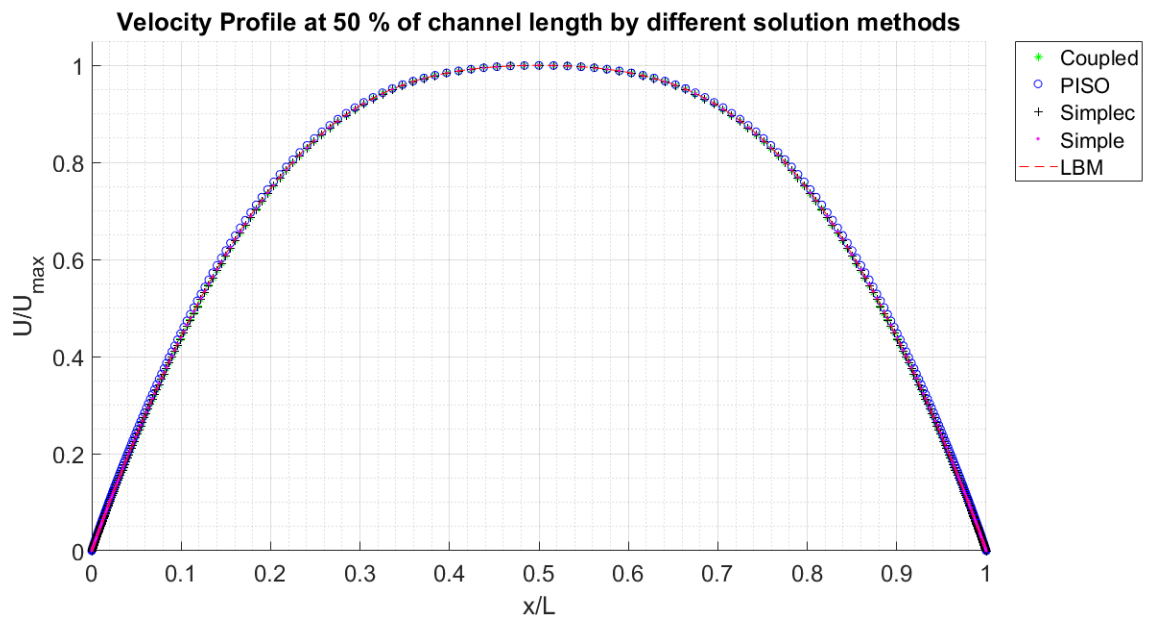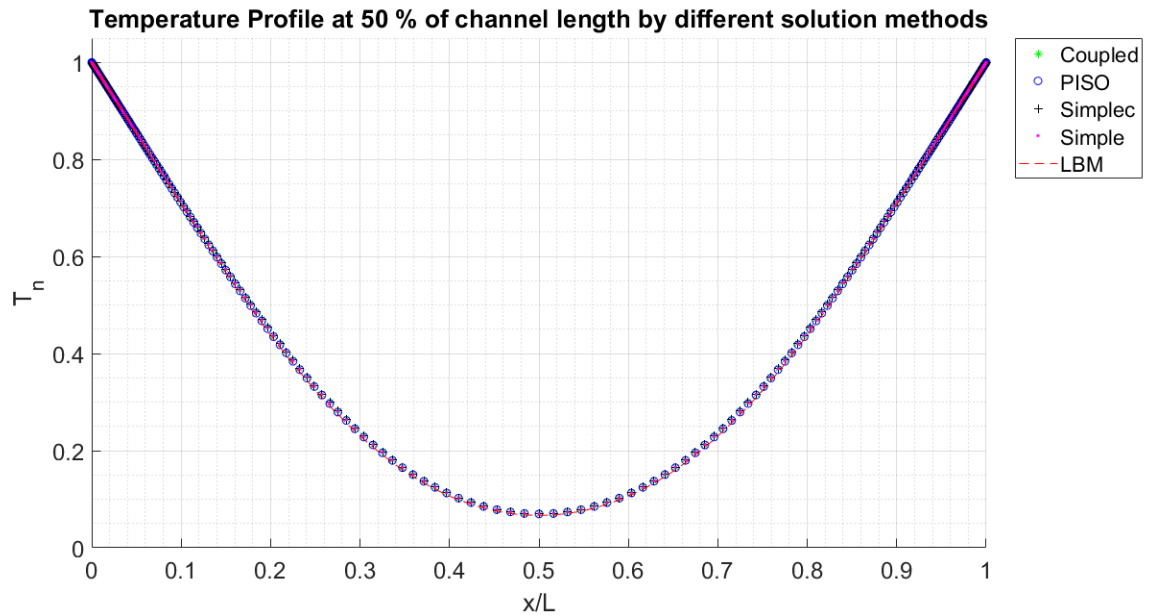Figure 3.15: Temperature profile comparison at 50% of the channel length
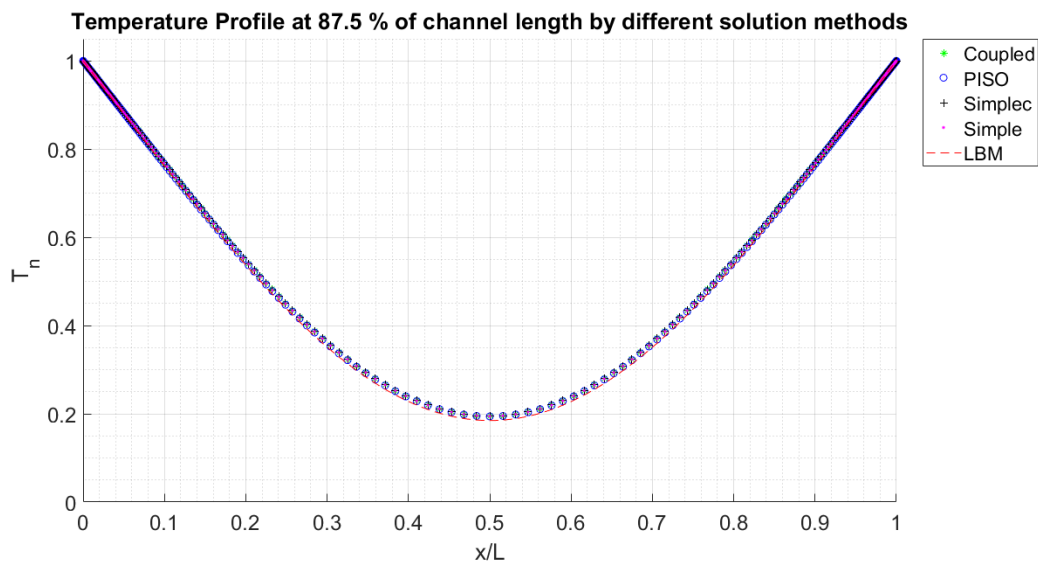
Figure 3.16: Temperature profile comparison at 87.5% of the channel length

The velocity profile obtained from the refined mesh showed better agreement with the LBM results. While taking a closer look at the percentage differences between the coupled and LBM for both identical and refined mesh, it can be stated that refined mesh results in a velocity profile that is much close to the LBM result. The closeup image of the velocity profiles of both identical and refined mesh at the mid section(50% of the channel length) can be seen in Figures 3.17 and 3.18. The difference in percentage from LBM, reduced from 0.902% for identical mesh to 0.025% for the refined mesh. Though there is only 0.877% decrease in the deviation, it gains importance in microscopic scales as typical diameter of droplets in the combustor are expected to be in order of μm. The mesh refinement improved the FLUENT result in coupled solution scheme to bring it closer to the LBM velocity result. In addition to it, the run time for LBM solver to reach steady state estimated to be $4:19$ minutes where as in case of FLUENT, it took $19:35$ minutes with the same computational resources to reach steady state. Though it can be understood that the second order accuracy requires higher

computational time, four times longer run time of FLUENT solver highlights the efficiency of LBM in single phase flows.
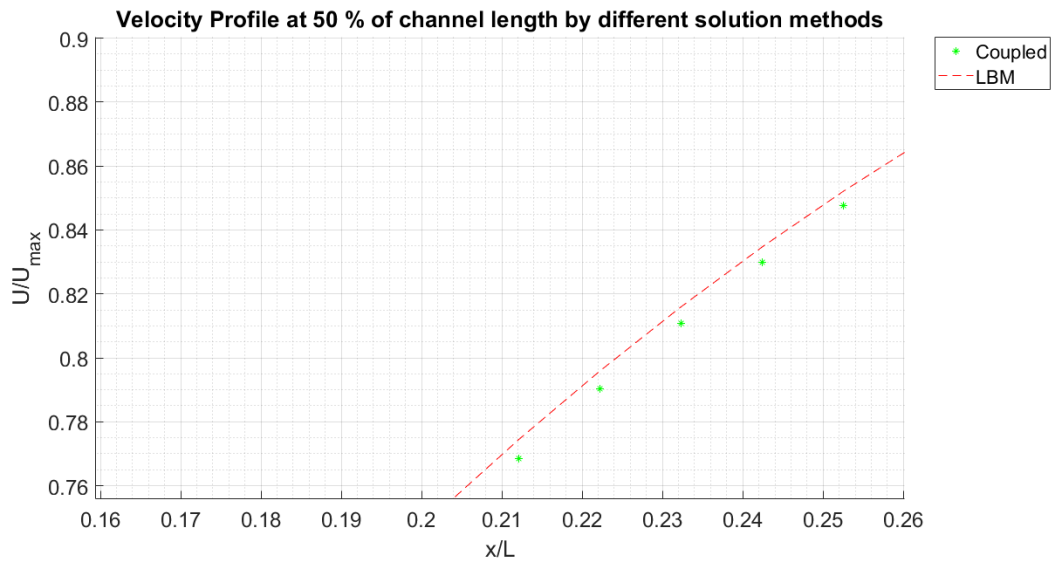
Figure 3.17: Zoomed Velocity profile comparison at 50% of the channel length, with Identical Mesh
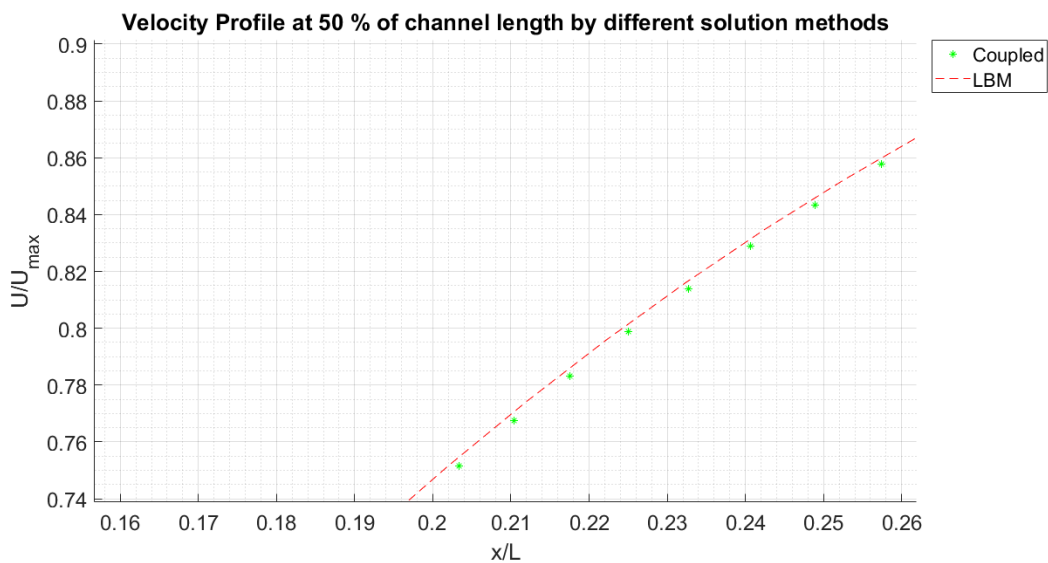
Figure 3.18: Zoomed Velocity profile comparison at 50% of the channel length, with Refined Mesh

In addition to the COUPLED scheme, the SIMPLE, SIMPLEC and PISO schemes also produced improved results in case of refined mesh. Though the identical mesh thermal profile results showed good agreement with the LBM results, increasing the mesh refinement did improve the agreement with LBM.

From the above discussion it can be concluded that,

LBM is in line with the most robust solution scheme for a single phase system available in FLUENT, in addition to the fact that it provides accurate and computationally efficient results with a coarse mesh than the recommended solution schemes for a simple single phase problem.

4

MULTI-COMPONENT/MULTI-PHASE LATTICE BOLTZMANN METHOD

This Chapter outlines the detailed research conducted for creating a multi-component Lattice Boltzmann Model. With the creation of LB methods, their application in multi-phase and multi-component flows is one of major topics of research [22]. The Lattice Boltzmann multi-component multi-phase method can be broadly classified into the following categories: *color-gradient LB method* [23], *free energy LB method* [24] and *pseudopotential LB method.*

Colour-gradient LB method
Colour-gradient LB method was developed by Gunstensen et al [23]. Gunsten employed different colours namely red and blue. They were used to represent binary fluids in a system. In addition to the standard collision operator, a sources term is employed like an added collision operator for generating surface tension. The separation of different phases and maintenance of interface requires a recolouring process [22].

Free-energy LB method
The free-energy LB method was proposed by Swift et al. [24]. This is based on thermodynamical considerations. Non-ideal thermodynamic pressure tensor was introduced into the second-order equilibrium density distribution function. Hence, the phase separation is defined by using EOS in the thermodynamic theory. The van der Waals EOS being one such example. The original free-energy model was limited due to the lack of Galilean invariance. Hence some correction terms had to be added to the equilibrium distribution function to restore the same [22].

The Pseudo-potential Model
The Pseudo-potential Model is the simplest multi-phase LB method and was originally developed by Shan and Chen [25]. The fluid interactions are mimicked by an interparticle potential, which enables fluid to separate automatically into phases or components without incorporation of interface tracking techniques. The Pseudo-potential LB method is a very popular multi-component multiphase method due to its conceptual simplicity and computational efficiency [22].

In this research work the Pseudo-potential LB method was used to create a multi-component fluid solver that can predict fluid properties at transcritical state. While simultaneously highlight the difficulties, advantages and the numerical problems associated with it.

4.1. ORIGINAL SHAN AND CHAN PSEUDO-POTENTIAL MODEL

The simplicity, versatility and auto phase or component separation of Pseudopotential model has made it one of the most popular schemes for multi-phase multi-component LBM [12]. It can handle different Equations of state, as well as include the fluid wettability while incorporating fluid contact angle. The original Shan and Chan model was proposed to simulate multi-phase and multi-component flow systems.

Microscopically, the separation of fluid system into components and phases is due to the inter-particle forces [13]. The simple long-range molecular(non-bonded interaction between molecules separated by considerable distance larger than the mean free path) interaction can be mimicked by interaction force between particles at node x and the particles at node x'(where x and x' are neighbouring sites in lattice system) is formulated as follows [12]:

$$F_f(x) = -\psi(x)\Sigma_{x'}G(x,x')\psi(x')(x'-x) \tag{4.1}$$

where $G(x,x')$ is Green's function and it satisfies $G(x,x') = G(x',x)$, highlighting the fact that interparticle strength between two different chemical component will be equal. It represents the inter-particle interaction, with $G(x,x') > 0$ indicating repulsive force between immiscible components and $G(x,x') < 0$ represents the attraction between particles of the same component. $\psi(x)$ is called the 'effective mass' and at a given location can be related to the local properties such as density,$\psi(x) = \psi(\rho)$,temperature and pressure based on the equation of state considered. The effective mass plays a vital role in Shan and Chan Pseudopotential model as it can be varied to incorporate different equations of state based on the system under study.

In order to simplify the application for numerical modelling, SC only considers the nearest neighbour inter-particle force, but with further development of the SC model Equation 4.1 is modified to include the next nearest neighbour nodes with the criteria that the as long as the gradient of effective mass term $\nabla\psi(x)$ is properly specified [12]. Hence the interaction strength for the nearest and next to nearest neighbours is given by Equation 4.2:

$$G(x,x') = \begin{cases} g, & |x-x'| = 1 \\ g/4, & |x-x'| = \sqrt{2} \quad\quad [12] \\ 0, & otherwise \end{cases} \tag{4.2}$$

The inter-particle force shown in Equation 4.1 can be written as shown in Equation 4.3 and the gradient of ψ, with the nearest and next nearest neighbours can be discretized as shown in Equations 4.4 and 4.5 for a lattice arrangement of $D2Q9$.

$$F_{int}(x) = -G\psi(x)\Sigma_{i=1}^{n} w_i\psi(x+e_i\Delta t)e_i \tag{4.3}$$

$$\frac{\partial\psi(i,j)}{\partial x} = c_1[\psi(i+1,j)-\psi(i-1,j)] + c_2[\psi(i+1,j+1)-\psi(i-1,j+1)+\psi(i+1,j-1)-\psi(i-1,j-1)] \; [12] \tag{4.4}$$

$$\frac{\partial\psi(i,j)}{\partial y} = c_1[\psi(i,j+1)-\psi(i,j-1)] + c_2[\psi(i+1,j+1)-\psi(i+1,j-1)+\psi(i-1,j+1)-\psi(i-1,j-1)] \; [12] \tag{4.5}$$

where c_1 and c_2 are the weighting coefficients for the corresponding nearest and next nearest nodes [12]. With the interaction of force represented in Equation 4.3 and combination based on Chapman-Enskog expansion, the EOS in LB method is given by:

$$P = c_s{}^2\rho + \frac{c_0}{2}G[\psi(\rho)]^2 \tag{4.6}$$

where c_s is the speed of the sound in the Lattice system. For the $D2Q9$ and $D3Q19$ models, the speed of sound is $c_s = \frac{1}{\sqrt{3}}$. The Equation 4.6 represents the non-ideal gas law, with the non-ideality depending explicitly on the fluid-fluid interaction. Generally the effective mass in Shan and Chan can be calculated as $\psi(x) = \rho_0[1 - exp(\rho/\rho_0)]$, which gives pressure density relationship, where ρ_0 is the reference density. The effective mass $\psi(x)$ can also be designed to incorporate different equations of state that will be discussed in Section 4.1.1. In addition to the forcing caused by the inter-particle interaction, addition forcing is added due to interaction of fluid with the solid walls F_{wall} and they will be explained in Section 4.3.

In the SC method, the inter-particle fluid force is incorporated into the model by via the equilibrium velocity shown in Equation 4.7. Hence the velocity u in Equation 2.18

$$u^{eq} = u + \frac{\tau F_{total}}{\rho(x)} \tag{4.7}$$

where $F_{total} = F_{int} + F_{wall}$. Then, by averaging the moment before and after the collision the whole fluid velocity U is given as :

$$\rho(x)U = \rho(x)u + \frac{1}{2}F_{total} \tag{4.8}$$

4.1.1. EFFECTIVE MASS

The relationship between pressure, temperature and density for a given substance is defined by the Equation of state (EOS). Ideal gas equation is given as $P = n\rho RT$. Although the relation seems accurate for gases at low pressure and temperature, the non-idealities that arise at high pressure renders the equation inaccurate.

The general idea is to associate the effective mass with different Equation of state. From Equation 4.6 the effective mass can be rewritten as follows:

$$\psi = \sqrt{\frac{2}{gc_s{}^2}(p - \rho c_s{}^2)} \tag{4.9}$$

It was proposed by Qin [26] to incorporate the required Equation of state into the Equation 4.9. For example in this research work van der Walls(vdW), the Equation 4.10 is incorporated into the effective mass calculation.

$$p = \frac{\rho RT}{1 - b\rho} - a\rho^2 \tag{4.10}$$

where a and b are the vdW parameters. At the critical point the first and second order derivative of pressure is zero [27], hence from Equation 4.10 and Equation 4.6 can be used to set the critical values of the interaction strength g,i.e. $\frac{\partial P}{\partial \rho} = 0$ and $\frac{\partial^2 P}{\partial^2 \rho} = 0$. Hence we can obtain the critical density ρ_c and the corresponding critical strength g_c as follows:

$$\rho_c = \rho_0 \ln 2 \tag{4.11}$$

$$g_c = -\frac{2}{9\rho_0} \tag{4.12}$$

.

This limit plays a vital role while defining the interaction strength for fluids at subcritical and supercritical state.

4.2. FLUID-FLUID INTERACTION

In multi-component systems one must also take into account the interaction between the components(inter) and within components(intra), including additional forcing terms. This section will detail out the forcing schemes for inter and intra components.

Presence of more than one chemical compound adds a great deal of complexity in the dynamics of the system.In LBM separate PDFs can be used to define each chemical compound. For a system with binary immiscible fluid A,B $f_{k,A}$ represents component A and $f_{k,B}$ represents component B. Each PDFs are evaluated separately with separate sets of streaming and collision steps. And the interaction between the fluids are incorporated through the $F_{k,int}$. The individual first and second order moments will represent the density and velocity vector of the corresponding component.

$$\rho_{A,lu} = \Sigma f_{k,A} \tag{4.13}$$

$$\rho_{B,lu} = \Sigma f_{k,B} \tag{4.14}$$

$$\rho_{A,lu} \, u_{A,lu} = \Sigma f_{k,A} c_k \tag{4.15}$$

$$\rho_{B,lu} u_{B,lu} = \Sigma f_{k,B} c_k \tag{4.16}$$

The subscript lu indicates the parameters are calculated in Lattice units. The transition of physical to lattice units was introduced in Section 2.3. As already stated, in a Multi-component system two types of particle interaction can be experienced, inter and intra. The inter-component interaction of Component A due to Component B creates an inter-component force that takes a generalized form:

$$F_{A,B} = -\psi_A g_{A,B} \nabla \psi_B \tag{4.17}$$

This forcing is present in addition to the intra component force created due to the interaction of particles within component A. It can be formulated as Equation 4.18:

$$F_{A,A} = -\psi_A g_{A,A} \nabla \psi_A \tag{4.18}$$

The parameters $g_{A,A}$ and $g_{A,B}$ are interaction strengths where the inter-particle strength $g_{A,B}$ is always chosen to be positive indicating the repulsion between immiscible components and the intra particle strength is taken negative to indicate attraction between particles of the same component. Usually the inter-component interaction strength for both the components are considered to be equal, $g_{A,B} = g_{B,A}$. The total force acting on component A and component B due to inter and intra particle interaction can be stated as follows:

$$\boldsymbol{F_{A,int}}(X) = -g_{A,A}\psi_A(X)c_s^2 \sum_{k=1}^{N} w(|e_k|^2)\psi_A(x+e_k\Delta t)e_k - g_{A,B}\psi_A(X)c_s^2 \sum_{k=1}^{N} w(|e_k|^2)\psi_B(x+e_k\Delta t)e_k \tag{4.19}$$

$$\boldsymbol{F_{B,int}(X)} = -g_{B,B}\psi_B(X)c_s^2 \sum_{k=1}^{N} w(|e_k|^2)\psi_B(x+e_k\Delta t)e_k - g_{B,A}\psi_B(X)c_s^2 \sum_{k=1}^{N} w(|e_k|^2\psi_A(x+e_k\Delta t)e_k \tag{4.20}$$

Hence the F_{total} for each Component will be given as

$$F_{total,A} = F_{A,int} + F_{A,wall} \tag{4.21}$$

In the equilibrium velocity calculation (as given by Equation 4.7), the velocity u for Multi-component system is calculated based on weighted density. This is considered to be common velocity for each component. It can be formulated as shown in Equation 4.22 [28], where i is the number of components in this equation:

$$u' = \frac{\sum_{i=1}^{N} \rho_i u_i \tau_i}{\sum_i \rho_i \tau_i} \tag{4.22}$$

4.3. FLUID-SOLID INTERACTION

The fluid solid interaction is calculated similar to the inter-component force calculation. It plays a vital role in case of wetting phenomena and setting contact angle but both are outside the scope of the thesis. Thus a general formulation is given in Equation 4.23 without diving further into this topic.

$$F_{wall} = -g_w \psi(\rho) \nabla s(x)) \tag{4.23}$$

The parameter s is set to 1 in presence of wall and 0 otherwise. The g_w is the interaction strength determining the wettability of the fluid with the wall.

4.4. NON-ZERO DENSITY NODES

As explained in Section 4.2 each component information is defined by separate PDF's. The nodes where component A is absent , cannot be set to zero as it might cause numerical instability and simulation crashes. Hence precious work on Multi-component LBM replaced the non-zero density nodes with negligible density values $0.001 \times \rho_A$, [28][29][12]. In this research work the zero density nodes is not replaced by negligible value. Instead the equilibrium velocity u^{eq} of component A is set to zero at nodes where the fluid density of component A is zero, it is supported by the idealogy that no fluid is present at that point to propagate the velocity.

4.5. THERMAL MULTI-COMPONENT/MULTI-PHASE MODEL

Incorporation of thermal model into the Mutli-component LB system is still under development and admittance of thermal variations leads to complications with the inter-component inter particle interaction parameters. The dependence of thermal model with the density model is similar to that explained in Section 2.7. One particular issue arises in the relation of thermal lattice temperature of a component to the macroscopic Temperature. This section gives a brief explanation of the Thermal Multi-component system.

4.5.1. MACROSCOPIC VARIABLE RECONSTRUCTION

For a system of binary immiscible fluids with thermal and multi-component effects, four separate PDFs must be considered. Two PDFs defining the hydrodynamics and two PDFs defining the thermodynamics of each component. The Equations 4.15 and 4.16 show that the separate velocities are evaluated for each component, but to the idea that these occur on overlapping spacial nodes of the two numerical grids (i.e. at the same spatial location). Hence the same procedure is adopted for the temperature, meaning if a system of cold droplet is surrounded by heated fluid, the two temperature PDFs separately evaluate the temperature fields for the same overlapping nodes. This causes an issue as it is not physically consistent for the same point or node in space to have multiple velocity and temperature information [29]. Hence the major difficulty for multi-component thermal model arises in reconstruction of the macroscopic velocity and temperature information from multiple individual velocity and thermal information. The macroscopic velocity plays a vital role for the thermal model and the density models are coupled by the velocity as shown in Figure 2.5. The conversion of multiple temperature information to single macroscopic temperature is done by coupling the individual temperature of components.

Initially, thermal PDFs are calculated separately for each chemical component. Temperature coupling is done post streaming, using a density-weighted combination of the physical temperature [29] as given by Equation 4.24:

$$T_{coupled,p} = \frac{\Sigma_{i=1}^{N} \rho_{i,p} T_{i,p}}{\Sigma \rho_{i,p}} \tag{4.24}$$

where the subscript p denotes that the variables are calculated in physical units and i stands for the chemical components. In binary immiscible fluid system (Component A and Component B), The couple temperature becomes (Equation 4.25:

$$T_{coupled,p} = \frac{\rho_{A,p} T_{A,p} + \rho_{A,p} T_{A,p}}{\rho_{A,p} + \rho_{B,p}} \tag{4.25}$$

where the physical values are computed from the macroscopic variables in the lattice domain, which are indeed computed from the corresponding PDFs similar to Equation 4.13 and 4.14:

$$T_{A,lu} = \sum_{k=1}^{n} g_{k,A} \tag{4.26}$$

$$T_{B,lu} = \sum_{k=1}^{n} g_{k,B} \tag{4.27}$$

The conversion of lattice units to physical units is done with respect to the critical parameters of the fluid system under consideration:

$$\rho_{A,p} = \rho A, lu \frac{\rho_{c,p}}{\rho_{c,LU}} \tag{4.28}$$

$$\rho_{B,p} = \rho B, lu \frac{\rho_{c,p}}{\rho_{c,LU}} \tag{4.29}$$

$$T_{A,p} = T_{B,lu} \frac{T_{c,p}}{T_{c,LU}} \tag{4.30}$$

$$T_{A,p} = T_{A,lu} \frac{T_{c,p}}{T_{c,LU}} \tag{4.31}$$

It is of vital importance to compute $T_{coupledp}$ in physical units rather than lattice temperature units for maintaining thermodynamic consistency. The major reason for this becomes clear when we look into the fact that the critical temperatures of each chemical component might be different hence resulting in different lattice temperatures. The coupled temperature for each respective component can be converted from physical units to lattice units post-coupling [29]. The conversion of $T_{coupled,p}$ to the respective components can be done as follows:

$$T_{A,coupled,lu} = T_{coupled,p} \frac{T_{c,lu}}{T_{c,p}} \tag{4.32}$$

$$T_{B,coupled,lu} = T_{coupled,p} \frac{T_{c,lu}}{T_{c,p}} \tag{4.33}$$

The critical values of the macroscopic parameters can be estimated from the EOS which is implemented in estimation of the effective mass as show in Section 4.1.1, which indeed are used to compute the intra-component and inter-component potentials. The velocity calculated from the two hydrodynamic PDFs must also be coupled [29] in such a way that the moment of the system is conserved globally, at the same time also maintaining consistency similar to the case of coupled temperature. The coupled velocity for the thermal PDFs can be computed as follows:

$$u_{coupled,lu} = \frac{\sum\limits_{i=1}^{N} \rho_{i,lu} u_{i,lu}}{\sum\limits_{i=1}^{N} \rho_{i,lu}} \tag{4.34}$$

This single coupled velocity is then used in the estimation of equilibrium distribution function of the corresponding components. Hence the equilibrium equation with the coupled velocity and temperature will be formulated as follows:

$$g_{k,A}^{e} q = w_k T_{A,coupled,lu} \left[1 + e_k.u_{coupled,lu} + \frac{1}{2}(e_k.u_{coupled,lu})^2 - \frac{1}{2} u_{coupled,lu}^2 \right] \tag{4.35}$$

$$g_{k,B}^{e} q = w_k T_{B,coupled,lu} \left[1 + e_k.u_{coupled,lu} + \frac{1}{2}(e_k.u_{coupled,lu})^2 - \frac{1}{2} u_{coupled,lu}^2 \right] \tag{4.36}$$

This equilibrium function gets incorporated in the collision term of the thermal PDFs separately for each component. The consistency of this approach is due the fact that the particles considered to be occupying same spatial nodes must equilibrise towards the same thermal equilibrium in the physical domain [29]. By ensuring immisicibility of the components the created thermal component will be able to simulate temperature gradient between two components.

5

VERIFICATION OF MULTI-COMPONENT LATTICE BOLTZMANN MODEL

This chapter reports the results obtained from multi-component LBM solver inclusing the verification with commercial fluid dynamic solver.

5.1. MULTI-COMPONENT HYDRODYNAMIC SYSTEM SET UP

Using the pseudo-potential forcing scheme, a multi-component LB model was created in MATLAB. The model validity is limited to the density ratio. The value is close to unity .i.e. $\frac{\rho_A}{\rho_B} = 1$. Two fluids namely castor oil and silicone oil were selected as the ideal candidates for verification of the LBM solver.

5.1.1. DOMAIN SPECIFICATION

A 2-D square of dimensions $0.301 \times 0.301 m$ is considered to be filled with silicone oil as primary fluid and the centre is filled by castor oil, secondary fluid. The L/D ratio of the system 5.01. The Physical fluid properties and domain specifications are converted to Lattice units as follows:

Domain dimension, $L_p = 0.301 \times 0.301 m$. In Lattice domain specification, the whole domain is discretized as 301×301 spatial node with each grid size equal to unity, i.e. $\Delta x = 1$. Hence the domain specification in lattice unit can be written as $L_{lu} = 301 \times 301 \ lu$. From the above data the conversion factor can be computed as follows:

$$C_l = \frac{L_p}{L_{lu}} = \frac{0.301}{301} = 10^{-3} m \tag{5.1}$$

The density of castor oil and silicone oil is $960 \ kg/m^3$ and $970 \ kg/m^3$ respectively, thereby having a density ratio of $\rho_A/\rho_B = 0.989$. The kinematic viscosity of castor and silicone oil is $0.3505 \times 10^{-3} \ m^2/s$ and $0.8215 \times 10^{-3} \ m^2/s$ respectively [30]. The density and fluid properties in physical units were converted to lattice units by normalising it with the properties of silicone oil. The normalisation is done as follows:

$$\rho_{castor-oil,lu} = \frac{\rho_{castor-oil,p}}{\rho_{silicone-oil,p}} = \frac{960}{970} = 0.989 \ latticedensity \tag{5.2}$$

$$\rho_{silicone-oil,lu} = \frac{\rho_{silicone-oil,p}}{\rho_{silicone-oil,p}} = \frac{970}{970} = 1 \ latticedensity \tag{5.3}$$

$$v_{castor-oil,lu} = \frac{v_{castor-oil,p}}{v_{silicone-oil,p}} = \frac{0.0008125}{0.0003505} = 2.32 \ lu^2/lt \tag{5.4}$$

$$v_{silicone-oil,lu} = \frac{v_{silicone-oil,p}}{v_{silicone-oil,p}} = \frac{0.0003505}{0.0003505} = 1 \ lu^2/lt \tag{5.5}$$

Since the relaxation time is dependent on the kinematic viscosity of the fluid (v), the value is reduced by an order of 10 to maintain the relaxation time within the stability limits. The reduced viscosity of silicone oil and castor oil are 0.1 lu^2/lt and 0.232 lu^2/lt respectively. From the kinematic viscosity in lattice units, the C_t conversion factor for time of the LB system can be computed as follows:

$$C_t = \frac{v_{lu}}{v_p} \times C_l^2 = \frac{0.232}{0.0008125} \times 10^{-6} = 2.84 \times 10^{-4} \ s \tag{5.6}$$

The conversion factor for time, C_t defines the time step size that can be used in FLUENT to make a quantitative comparison of the results.

For verification of the hydrodynamic model, two test cases were considered. The first case is transition of a deformed droplet to steady-state and the second case is the study of droplet coalescence by keeping two spherical shaped droplet just in contact with each other and observation of formation into single large droplet due to surface tension.

5.1.2. ASSUMPTIONS

For the case of hydrodynamic multi-component model several assumptions were made:

- The system is isothermal hence the relaxation time for each component is constant through out the domain.

- The domain boundary is set to wall condition. Hence the bounce back scheme was applied on the four sides of the LB spatial domain.

- Two Dimensional Model.

5.1.3. FLUENT SET-UP

FLUENT has an inbuilt model set called the Volume of Fluid (VOF) that can simulate immiscible multi-fluids by solving a single set of momentum equations and tracking the volume fractions for each of the fluids in the given grid throughout the domain [21]. It is one of the prominent methods of liquid-gas or liquid-liquid interface tracking. It also requires the solver to be pressure-based. The major reason for using VOF method over Level Set is to ensure mass conservation and to avoid sudden change in the phase function near the interface. To counter the sharp change in phase function larger number of grid points is required, which in turn increases the computational cost [31]. The over all setup in FLUENT can be stated as follows:

- Solver Set up

  – Type - Pressure - Based
  – Time - Transient

- Model

  – Volume of Fluid (VOF)

- Solution Methods

  – Scheme : Coupled - Pressure velocity Coupling

- Time step size - $C_t = 2.88 \times 10^{-4}$

- Number of times steps differs for the test cases

In order to maintain uniformity the mesh created for FLUENT is identical to the LB spatial mesh, i.e. 301×301 cells including the time step.

5.1.4. TEST CASES

The pictorial representation of each of the test cases, results from both fluent and LBM are compared and reported in this section

DEFORMED DROPLET

In the 2-D LB spatial domain filled with silicone oil, at the centre castor oil is introduced with a square shape of side 54 lu and 0.054 m for the FLUENT case. This shape available in FLUENT as default shape and the square side was chosen to maintain the L/D ratio of 5.01. The simulation was run for 0.992s in both LBM and FLUENT, where 0.992 seconds is the characteristic time taken for a castor oil droplet to reach steady state. The pictorial representation of the process can be seen in Figure 5.1.
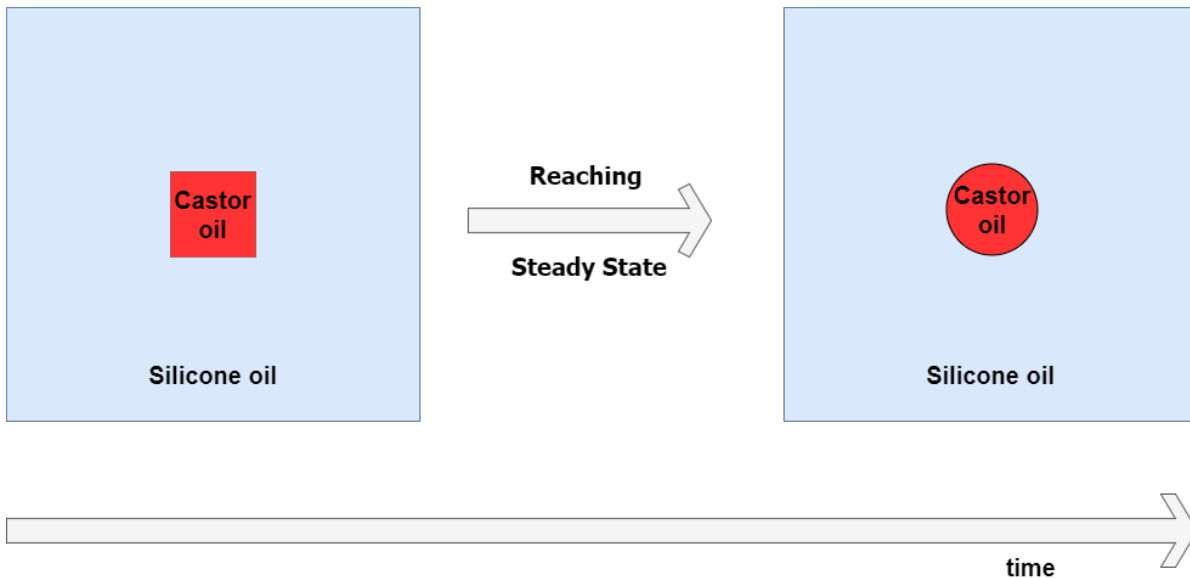

Figure 5.1: Pictorial representation of deformed droplet to steady state

Figures 5.2 and 5.3 show the initial system setup in LBM and FLUENT respectively. Figures 5.4 and 5.5 shows the comparison of density of castor oil and silicone oil (after reaching steady state) respectively at the mid line of the domain. Figures 5.6 and 5.7 show the domain after reaching steady state in LBM and FLUENT respectively.
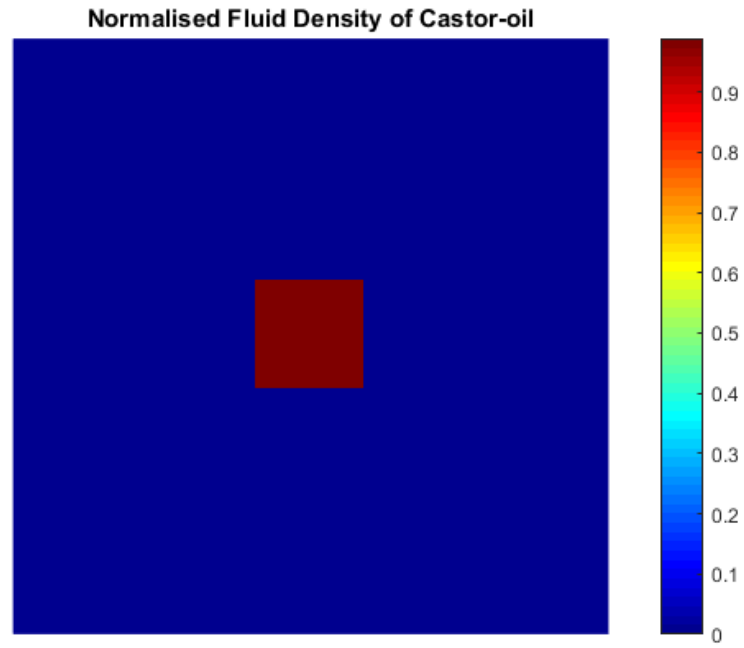
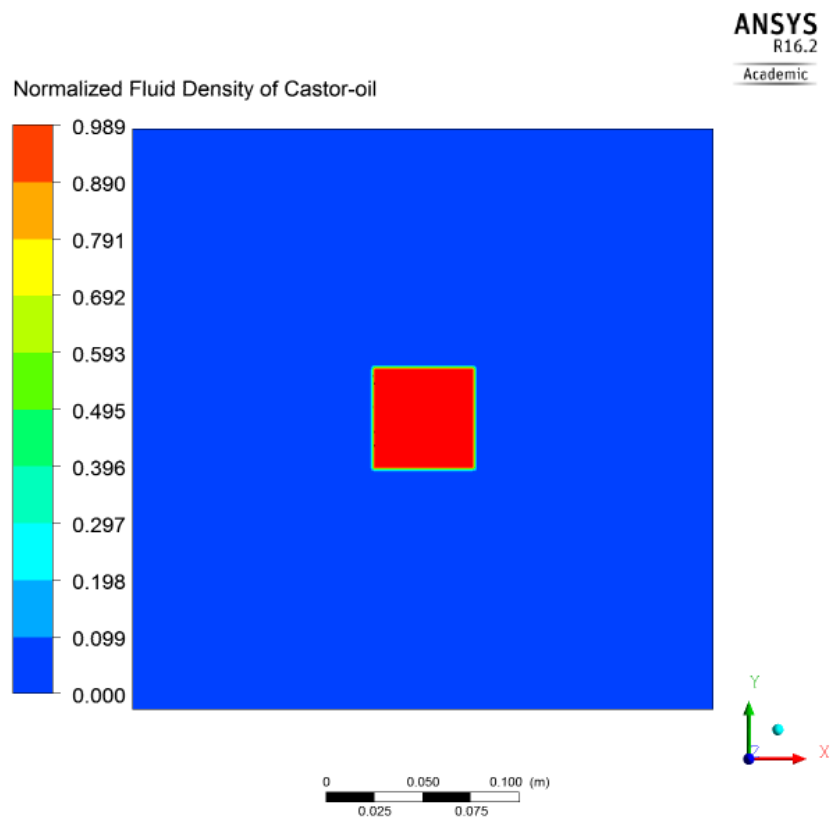Figure 5.2: Normalised density of Castor oil during initialisation

Figure 5.3: Normalized fluid density of Castor oil in FLUENT during initialisation
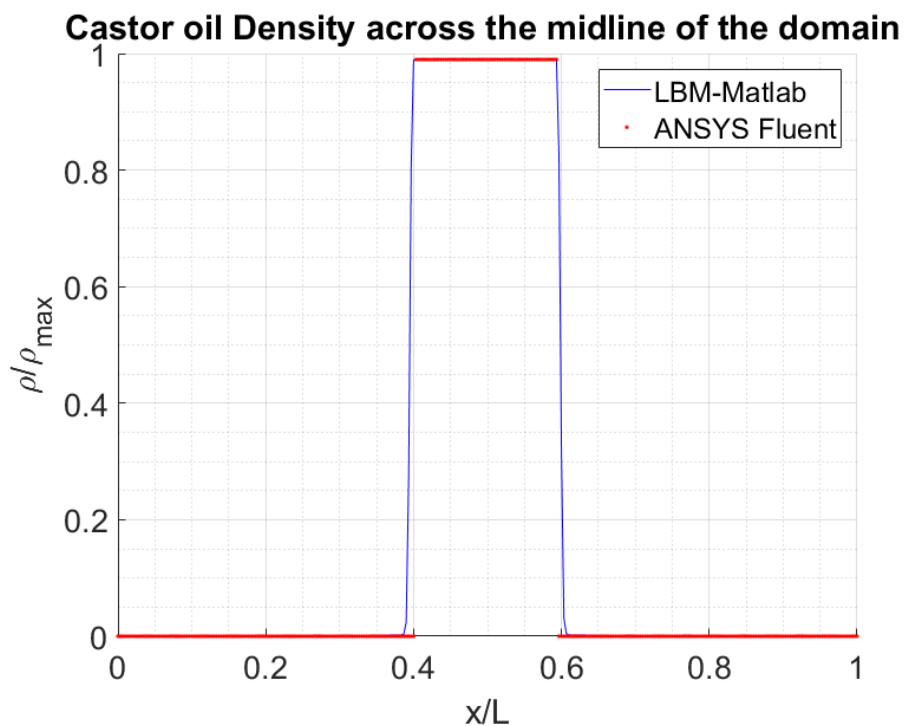
Figure 5.4: Normalized fluid density of castor oil comparison between FLUENT and LBM after reaching steady state
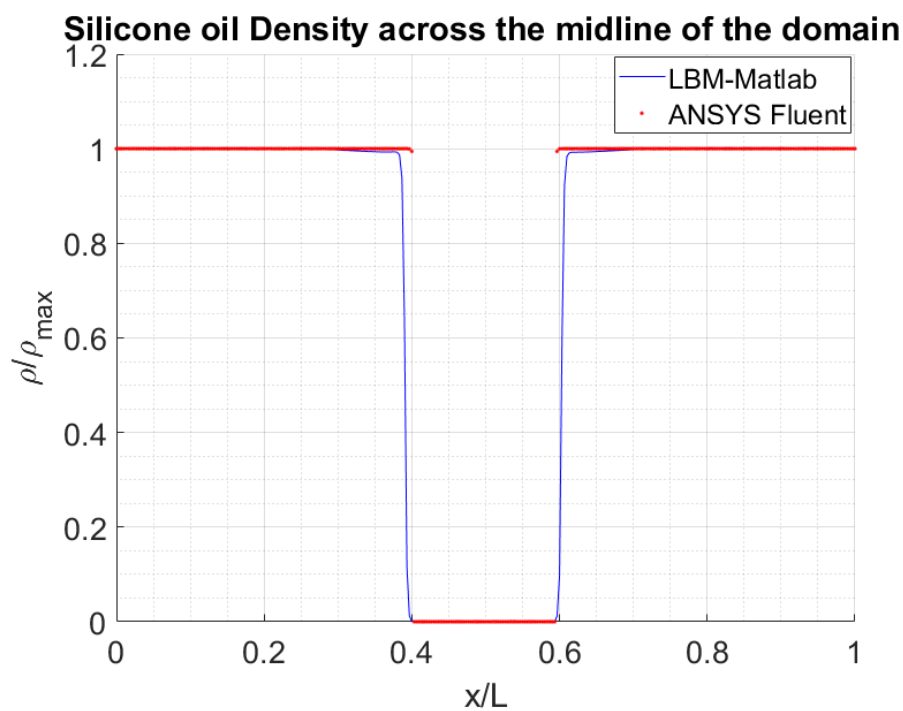

Figure 5.5: Normalized fluid density of silicone oil comparison between FLUENT and LBM after reaching steady state
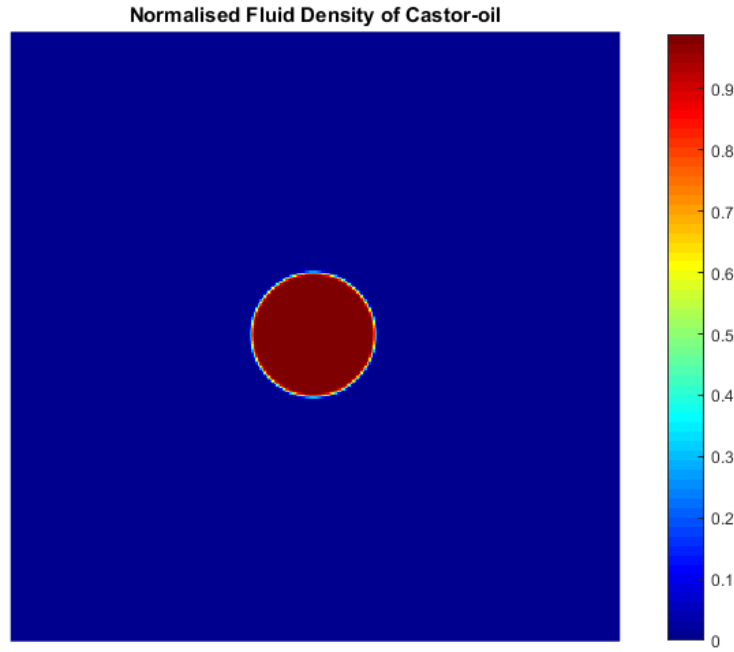
Figure 5.6: Normalized density of Castor oil after reaching steady state in LBM
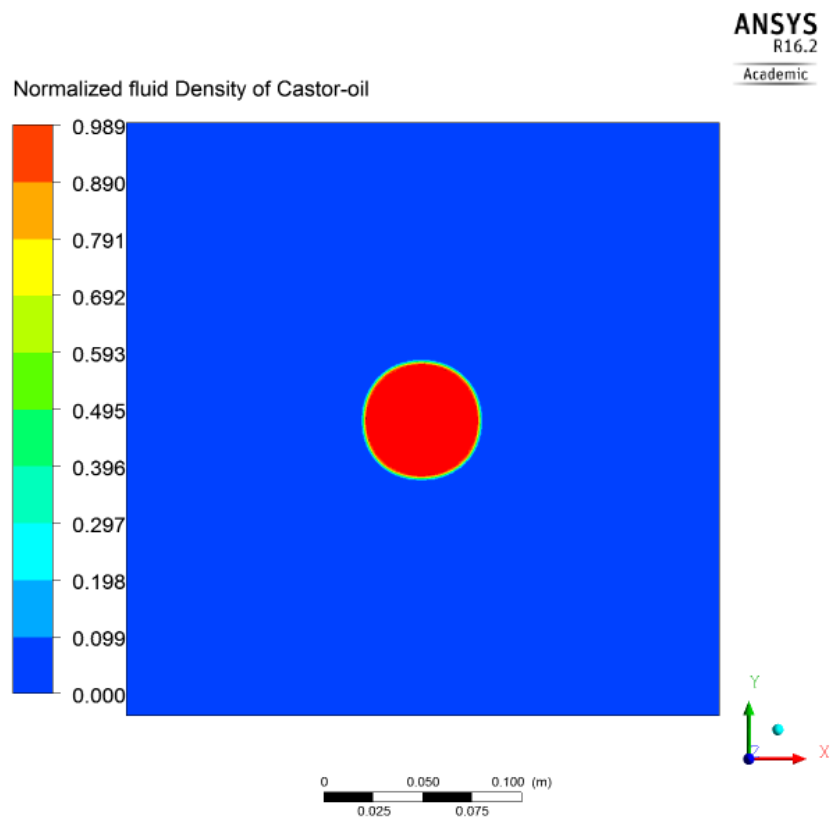

Figure 5.7: Normalized fluid density of Castor oil in FLUENT after reaching steady state

DROPLET COALESCENCE

For Droplet coalescence two droplets of castor oil of radius $30lu$ or $0.03m$ is kept in contact with each other and simulation is run expecting the droplet to combine to form one big droplet. The fluid properties and FLUENT set up are all the same except the time to reach steady state. Figure 5.9 and 5.10 shows the initial set up of LBM. Representation of the simulation can be seen in Figure 5.8. Figures 5.11 and 5.12 show the coalescence of two droplets at 70% and 100% of the characteristic coalescence time. Figure 5.13 shows the density of mixture in FLUENT after reaching steady state.
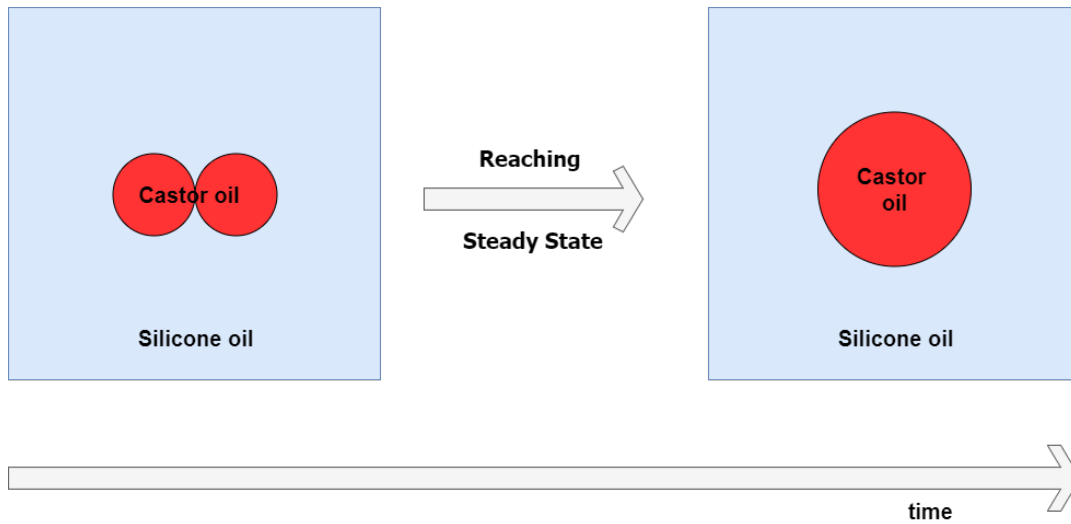

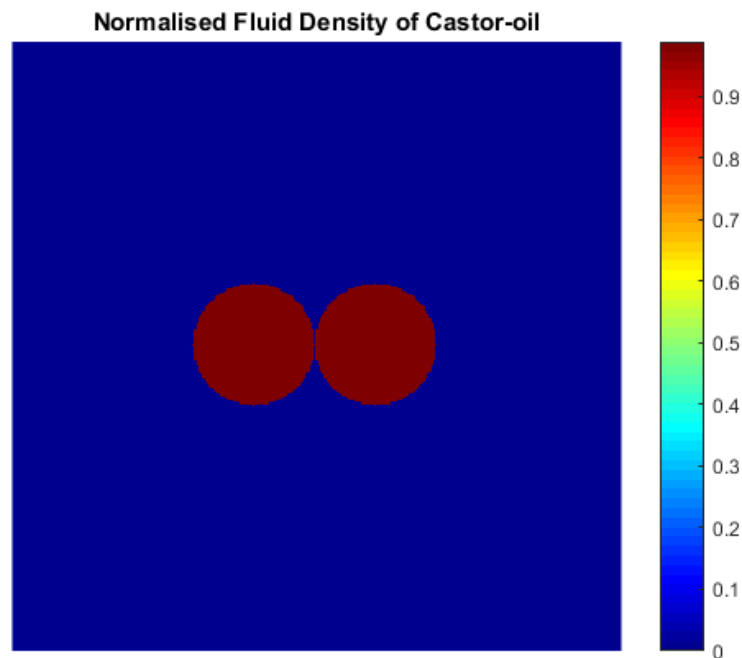Figure 5.8: Pictorial representation of droplet coalescence

Figure 5.9: Normalized fluid density of Castor oil in LBM at initialisation
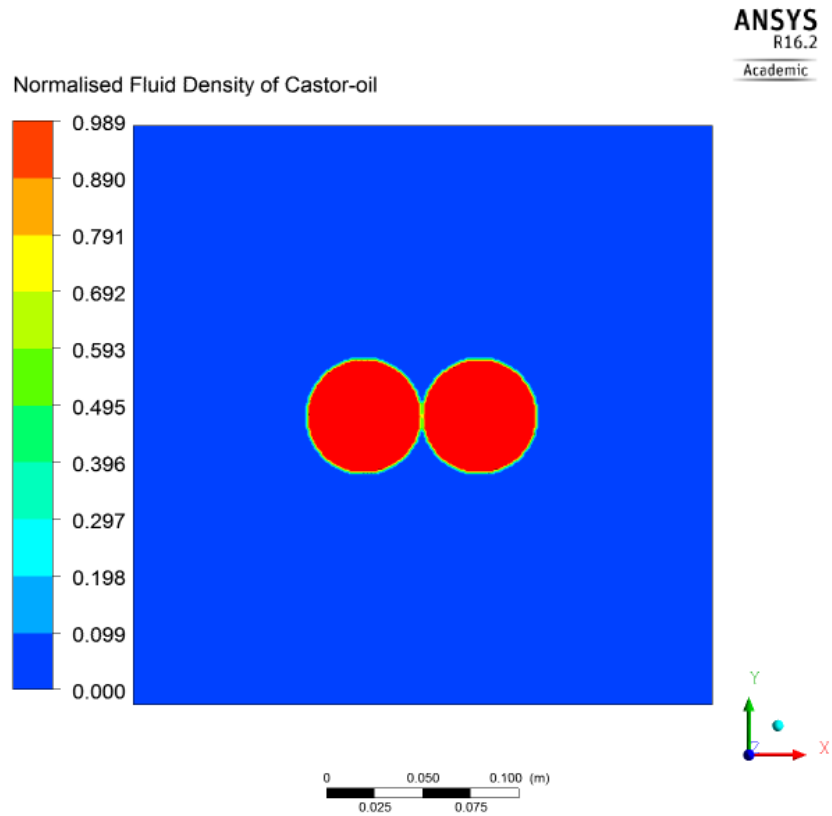
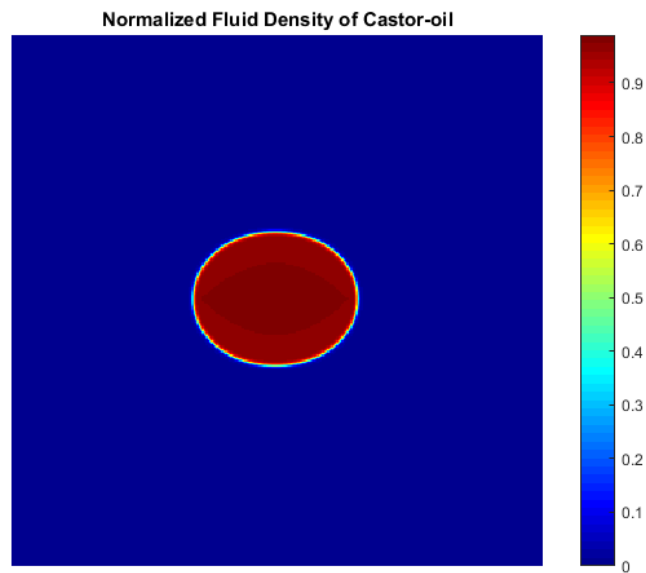Figure 5.10: Normalized fluid density of Castor oil in FLUENT at initialisation

Figure 5.11: Normalized fluid density of Castor oil in LBM at 70% of the characteristic time of coalescence
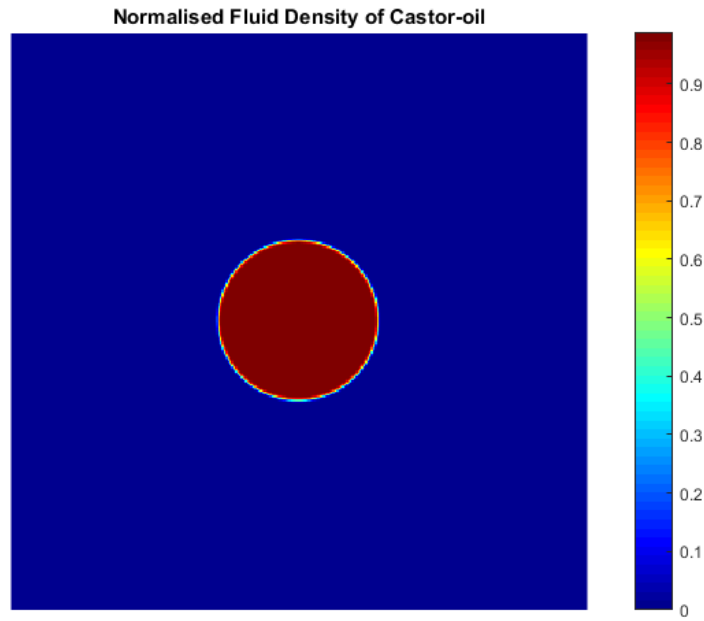
Figure 5.12: Normalized fluid density of Castor oil from LBM after reaching steady state
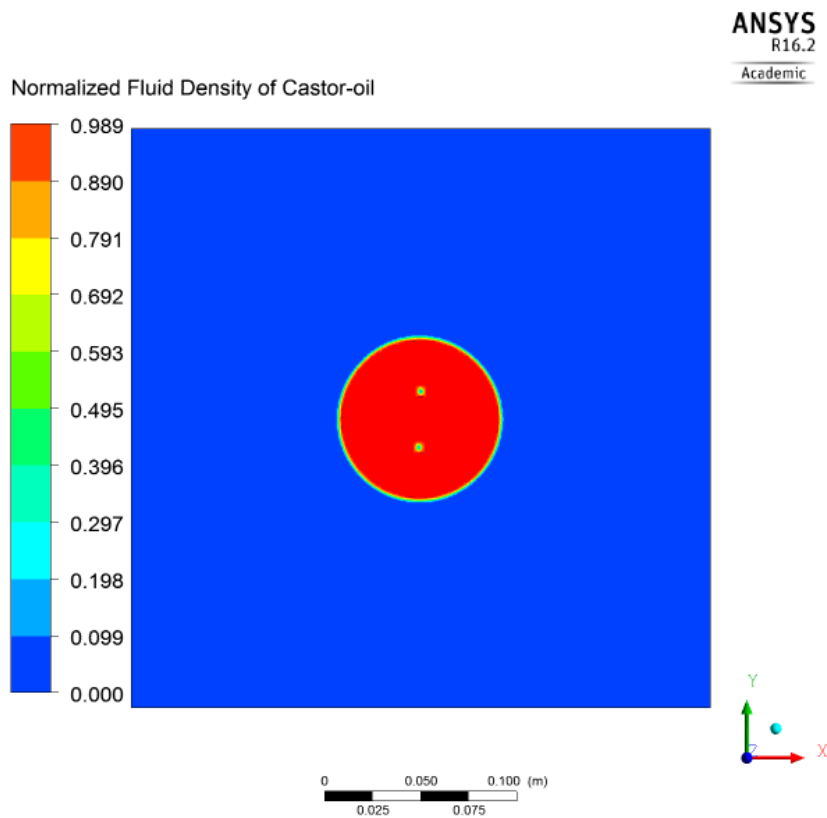

Figure 5.13: Normalized fluid density of Castor oil from FLUENT after reaching steady state

5.1.5. Observation and Discussion

From the results in the previous section it can be stated that LBM captures the physics of fluid in case of transition of deformed droplet to steady state and in the case of droplet coalescence. From the comparison plots in Figure 5.4 and 5.5 it can be seen that the LBM system is in good agreement with the FLUENT result with less than 1.5% diffusion in case of castor and silicone oil due to numerical diffusion, which can be further reduced by alerting the inter and intra component interaction strength.

In case of droplet coalescence it can be seen that large spherical droplet resulted in LBM simulations with no bubbles, i.e. no discontinuity in the fluid contour. In case of FLUENT a large spherical droplet with silicone oil trapped inside was formed.This supports the conclusion that when complex flow are to be modelled LBM can predict the fluid properties with better accuracy with a coarse mesh hence requires less computational cost.

5.2. Thermal Multi-component system set up

The multi-component system is limited to density ratio, and due to the lac of readily available data on oil properties.Two artificial fluids with properties of water at two different temperature were created and set to be immiscible fluids. More precise explanation can be seen as follows:

- Fluid 1 - Droplet at the centre of the domain

    - Density $\rho_{1,p} = 998\ kg/m^3$

    - Viscosity $v_{1,p} = 0.8 \times 10^-6\ m^2/s$

    - Prandtl Number $Pr = 5.43$

    - Temperature $T_A = 320K$

- Fluid 2 - primary fluid that fills the domain

    - Density $\rho_{1,p} = 992\ kg/m^3$

    - Viscosity $v_{1,p} = 0.553 \times 10^-6\ m^2/s$

    - Prandtl Number $Pr = 3.56$

    - Temperature $T_B = 350K$

- Since both the fluids properties are taken from water, the common critical parameters are follows

    - Critical Density $\rho_{cr} = 322\ kg/m^3$

    - Critical Temperature $T_{cr} = 647\ K$

- Domain specification ($L/D = 5$).

*All the fluid properties and critical parameters were obtained from **Refprop**.*
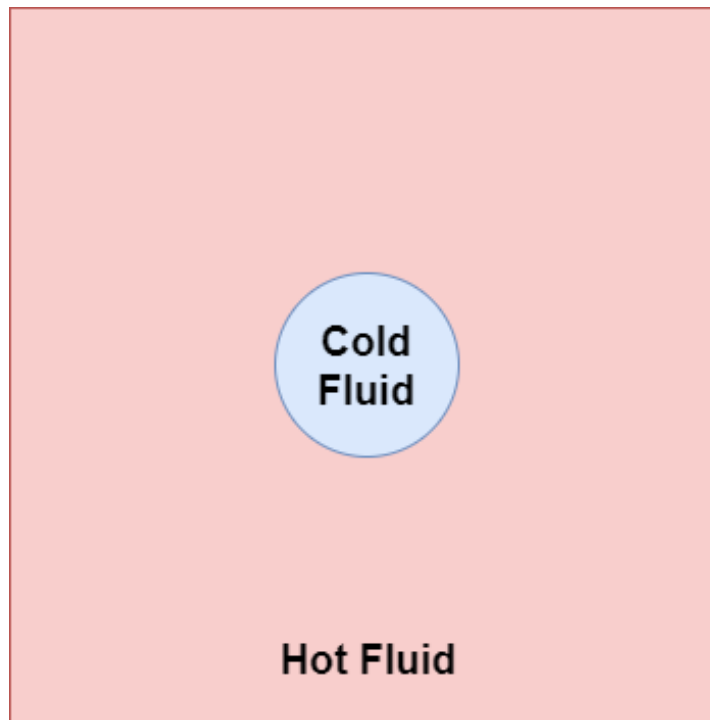
Figure 5.14: Pictorial representation of the thermal Multi-component model

Despite several attempts by adjusting the inter-particle strength, the Thermal model resulted in a temperature gradient with a small jump of 35% T_n from Equation 3.10, near the interface spike near the interface as shown in Figure 5.15. When attempted to reduce the spike, there was an improvement in the temperature gradient but with an increased diffusion in density as shown in Figure 5.16.

Figure 5.15: Reduced Density and Temperature at the mid section of the domain

Figure 5.16: Reduced Density and Temperature at the mid section of the domain

5.2.1. OBSERVATION AND DISCUSSION

From the Figures 5.15 and 5.16 it can be clearly seen that thermal multi-component results in a non-physical temperature distribution with a jump near the interface. This may be due to the following reasons:
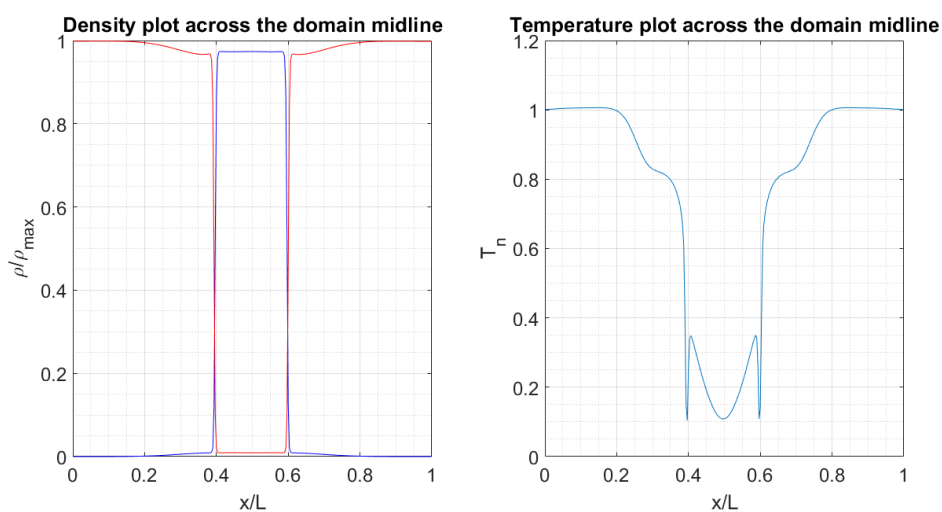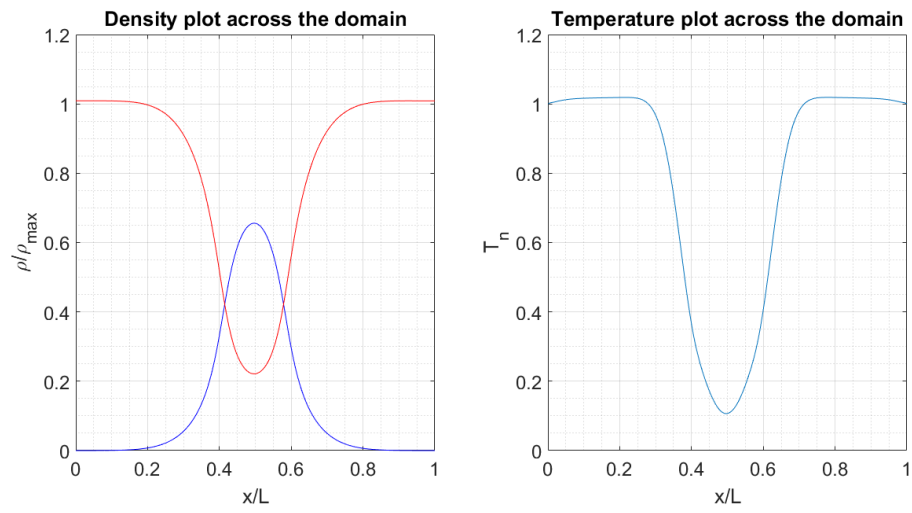
- The model cannot handle the sharp change in fluid properties across the fluid interface

- Additional forcing required to include the Soret Effect of the fluid.

- The implementation of equilibrium velocity u^{eq} to be zero at the zero density nodes.

The reduction in the interaction strength removed the temperature jump completely and resulted in a smooth thermal gradient. This might be a problem in case of immiscible fluids at sub-critical state. Where as fluids in supercritical state tend to be soluble in the surrounding medium due to its gas like diffusive property highlighted in the introduction chapter. It can be concluded that though the multi-component thermal model

has been created, it further requires improvement to make it robust and solve the issue with the temperature gradient spike near the interface which cannot be fulfilled in this research work due to time constraint.

6

CONCLUSION AND RECOMMENDATION

This chapter outlines the major contributions of this research work, followed by a set of recommendations for future works.

6.1. MAJOR CONTRIBUTIONS

- A single component/phase LBM has been devised and validated with all available pressure velocity coupling solution schemes in FLUENT. The comparison of results from LBM solver and FLUENT indicated that LBM yield accurate results with a coarser mesh. The COUPLED solution scheme having the minimal percentage difference of about 0.9% from the LBM results. The SIMPLE, SIMPLEC and PISO scheme had a percentage difference of 19.3%, 10% and 14.2% respectively. With mesh refinement the percentage difference between the FLUENT and LBM results reduced. The percentage difference between LBM and coupled solution scheme reduced from 0.9% to 0.025% with mesh refinement. Another advantage of LBM single component solver is that with the same computational resources the LBM solver reached steady state with about four times reduced wall clock time compared to the FLUENT solver.

- The newly created Multi-component hydrodynamic LBM solver showed formation of single large droplet in the case of droplet coalescence with out discontinuity. Discontinuity here refers to the presence of secondary fluid in the final droplet which was the result in case of the Fluid dynamic solver(FLUENT). The observation showcased that LBM solvers inherent advantage to define phase or component separation and capability to accurately simulate complex fluid flow.

6.2. CONCLUSION

- The computational time and accuracy of LBM solvers indicate an upper hand in using LBM as an effective alternative for single phase engineering problems. One of the shortcoming of the created single component LBM solver is the thermal(ω_T) and momentum(ω_ρ) relaxation time are constant throughout the domain instead of varying with respect to the fluid properties at each lattice node.

- The immiscible Multi-component hydrodynamic model though restricted by the density ratio performed in par and in certain cases more accurate than the commercial tool FLUENT. Thereby suggesting that LBM is more efficient and computationally inexpensive for complex flows such as droplet coalescence.

- For the test case of transition of deformed droplet to steady state LBM and fluid dynamic solver FLUENT performed on par with each other. The comparison of individual fluid density showed good agreement between FLUENT and LBM. The interface thickness is 1.47% larger in case of LBM due to the numerical diffusion that exists in the Shan and Chen methodology.

- Traditionally in multi-component LBM solver the zero density nodes are replaced with small numerical values to ensure the proper working of solver. In this research work instead of assumption of presence of small quantity of fluid in zero density nodes, the equilibrium velocity of the corresponding components in that lattice nodes are set to zero. The multi-component model created in this research work is free of numerical assumption for the sake of numerical stability. The implementation of setting the equilibrium velocity to zero is done with understanding of the basic physics, no fluid present at that spatial node to propagate the velocity to the neighbouring nodes. The density ratio limit of the multi-component LBM cripples the usage for variety of fluid combination that prevail in engineering application.

- The thermal immiscible multi-component model failed to capture the actual transport properties even at subcritical conditions. The observed jump in the temperature gradient across the interface showed that the thermal model cannot treat sharp interface with high inter-particle strength values. Lowering the inter-particle strength value results in density diffusion and smoothens the temperature. Hence the thermal model requires further work to make it more robust.

6.3. Recommendations for future work

- The current multi-component model is limited to density ratio near unity and the viscosity ratios less than 10. Hence the first qualitative step would be to upgrade the model to simulate higher range of density and viscosity ratios. It can be done by adopting Exact Difference Method (EDM) for modelling the fluid-fluid inter-particle forcing term.

- Application of EDM in thermal multi-component model may remove the temperature spike across the interface with high interaction strength values.

- The 2-D model can be extended to 3-D space easily with additional directional velocities and boundary conditions.

- The hydrodynamic model can be modified so as calculate the relaxation time at each lattice site based on the macroscopic fluid property at the corresponding lattice site.

BIBLIOGRAPHY

[1] A. Sieminski, *International energy outlook,* Energy Information Administration (EIA) (2014).

[2] S. Rahm, J. Goldmeer, M. Molière, and A. Eranki, *Addressing gas turbine fuel flexibility,* GER4601, General Electric (2009).

[3] J. E. Penner, *Aviation and the global atmosphere: a special report of ipcc working groups i and iii in collaboration with the scientific assessment panel to the montreak protocol on sustance that deplete the ozone layer,* (1999).

[4] J. Foster and R. S. Miller, *Fundamentals of high pressure combustion* (na, 2010).

[5] E. W. Lemmon, M. L. Huber, M. O. McLinden, *et al., Nist standard reference database 23,* NIST Reference Fluid Thermodynamic and Transport Properties—REFPROP, version **9**, 55 (2010).

[6] J. Yu and S. Eser, *Determination of critical properties (tc, pc) of some jet fuels,* Industrial & engineering chemistry research **34**, 404 (1995).

[7] *European aviation environmental report 2016,* (2016).

[8] T. S. Snyder, T. J. Rosfjord, J. B. McVey, and L. M. Chiappetta, *Comparison of liquid fuel/air mixing and nox emissions for a tangential entry nozzle,* (1994).

[9] B. Chehroudi, *Recent experimental efforts on high-pressure supercritical injection for liquid rockets and their implications,* International Journal of Aerospace Engineering **2012** (2012).

[10] G. Anitescu, L. L. Tavlarides, and D. Geana, *Phase transitions and thermal behavior of fuel- diluent mixtures,* Energy & Fuels **23**, 3068 (2009).

[11] L. L. Tavlarides and G. Antiescu, *Supercritical diesel fuel composition, combustion process and fuel system,* (2009), uS Patent 7,488,357.

[12] P. Yuan, *Thermal lattice Boltzmann two-phase flow model for fluid dynamics,* Ph.D. thesis, University of Pittsburgh (2006).

[13] Q. Kang, D. Zhang, and S. Chen, *Displacement of a two-dimensional immiscible droplet in a channel,* Physics of fluids **14**, 3203 (2002).

[14] K. Luo, J. Xia, and E. Monaco, *Multiscale modeling of multiphase flow with complex interactions,* Journal of Multiscale Modelling **1**, 125 (2009).

[15] A. A. Mohamad, *Lattice Boltzmann method: fundamentals and engineering applications with computer codes* (Springer Science & Business Media, 2011).

[16] J. Michael C. Sukop, Daniel T. Thorne, *Lattice Boltzmann Modelling: An introduction for Geoscientists and Engineers* (Springer Science & Business Media, 2007).

[17] J. Latt, *Choice of units in lattice boltzmann simulations,* Freely available online at http://lbmethod. org/_media/howtos: lbunits. pdf (2008).

[18] S. Succi, *The lattice Boltzmann equation: for fluid dynamics and beyond* (Oxford university press, 2001).

[19] J. Bao, *High density ratio multi-component lattice Boltzmann flow model for fluid dynamics and CUDA parallel computation,* Ph.D. thesis, University of Pittsburgh (2010).

[20] W. A. Sirignano, *Fluid dynamics and transport of droplets and sprays* (Cambridge University Press, 1999).

[21] F. Inc., *Pressure Velocity coupling,* https://www.sharcnet.ca/Software/Ansys/17.0/en-us/help/flu_th/flu_th_sec_uns_solve_pv.html (2017), [Online; accessed 28-October-2017].

[22] Q. Li, K. Luo, Q. Kang, Y. He, Q. Chen, and Q. Liu, *Lattice boltzmann methods for multiphase flow and phase-change heat transfer,* Progress in Energy and Combustion Science **52**, 62 (2016).

[23] A. K. Gunstensen, D. H. Rothman, S. Zaleski, and G. Zanetti, *Lattice boltzmann model of immiscible fluids,* Physical Review A **43**, 4320 (1991).

[24] M. R. Swift, W. Osborn, and J. Yeomans, *Lattice boltzmann simulation of nonideal fluids,* Physical review letters **75**, 830 (1995).

[25] X. Shan and H. Chen, *Lattice boltzmann model for simulating flows with multiple phases and components,* Physical Review E **47**, 1815 (1993).

[26] R. Qin, *Mesoscopic interparticle potentials in the lattice boltzmann equation for multiphase fluids,* Physical Review E **73**, 066703 (2006).

[27] L. Chen, Q. Kang, Y. Mu, Y.-L. He, and W.-Q. Tao, *A critical review of the pseudopotential multiphase lattice boltzmann model: Methods and applications,* International Journal of Heat and Mass Transfer **76**, 210 (2014).

[28] J. Bao and L. Schaefer, *Lattice boltzmann equation model for multi-component multi-phase flow with high density ratios,* Applied Mathematical Modelling **37**, 1860 (2013).

[29] M. Ikeda, P. Rao, and L. Schaefer, *A thermal multicomponent lattice boltzmann model,* Computers & Fluids **101**, 250 (2014).

[30] S. Mhatre, S. Deshmukh, and R. M. Thaokar, *Electrocoalescence of a drop pair,* Physics of Fluids **27**, 092106 (2015).

[31] J. A. Sethian and P. Smereka, *Level set methods for fluid interfaces,* Annual review of fluid mechanics **35**, 341 (2003).